UiT
THE ARCTIC
UNIVERSITY
OF NORWAY

Faculty of Engineering Science and Technology

Current Source Inverter for Battery Energy Storage System

Abdul Qudoos Mohammadi

Master's thesis in Electrical Engineering ELE-3900, May 2023

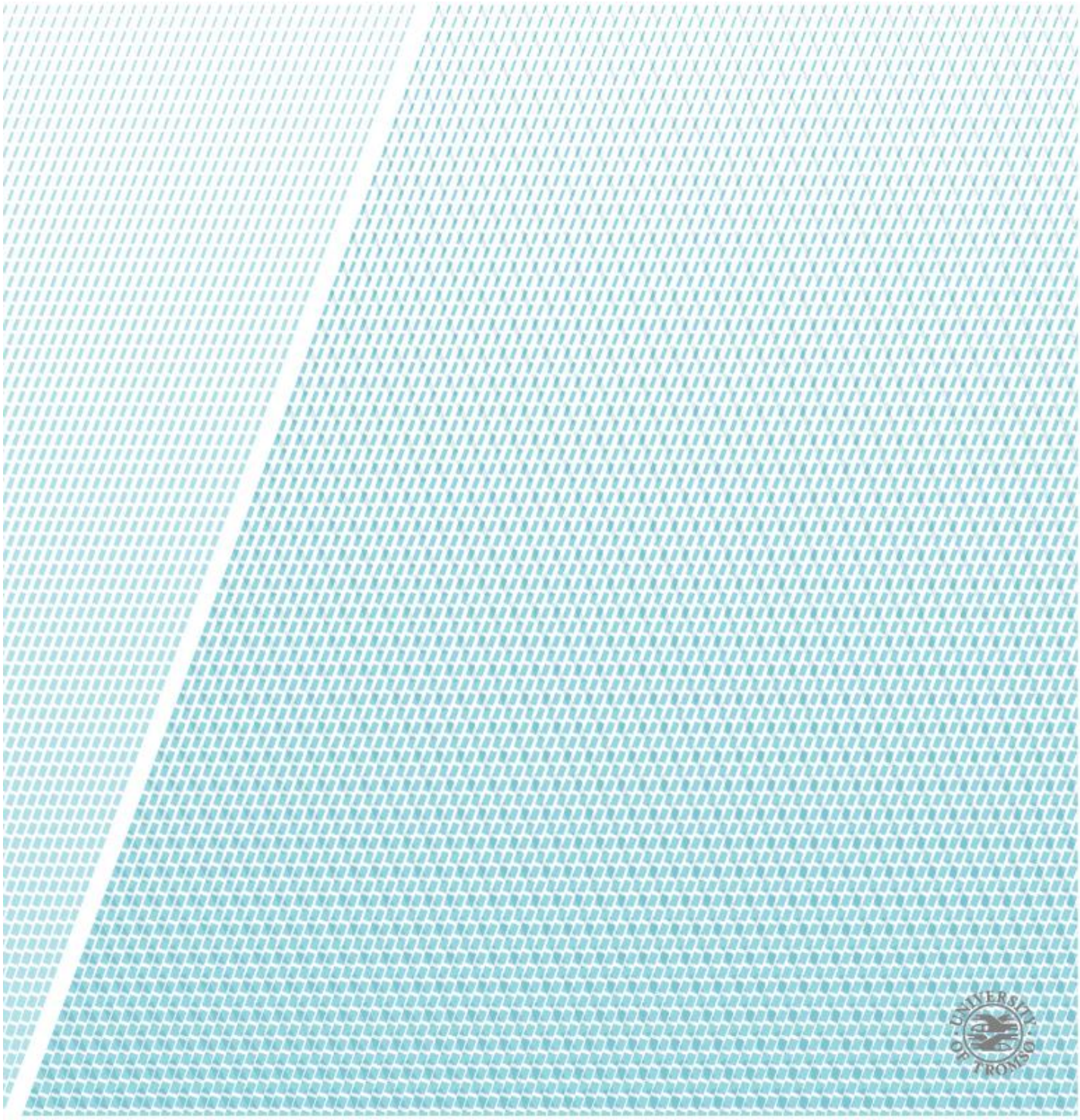

Current Source Inverter for Battery Energy Storage System

Submitted by: Abdul Qudoos Mohammadi

Supervisor: Umer Sohail

Co-supervisor: Trond Østrem

Submission: in May 2023

Master of Science in Electrical Engineering

Department of Electrical Engineering UiT-The Arctic University of Norway

Acknowledgment

This master's thesis concludes my two-year degree in electrical engineering at the Department of Electrical Engineering at UiT-The Arctic University of Norway. I would like to express my gratitude to my supervisor, Umer Sohail, PhD candidate at the Department of Electrical Engineering, UiT-The Arctic University of Norway, for their experienced guidance and general support, despite their busy schedules. Whenever I had doubts about some aspects of the theory or lacked self-confidence, his words motivated me and helped me keep my focus on this thesis. His help was priceless, as was his moral support. Furthermore, I would like to thank my co-supervisor, Trond Østrem, Associate Professor at the Department of Electrical Engineering at UiT-The Arctic University of Norway, for his support and guidance.

I would like to take this opportunity to thank my institute UiT-The Arctic University of Norway for funding my degree and giving me an opportunity to undertake this research at department of Electrical Engineering.

May 2023

Narvik, Norway

Abdul Qudoos Mohammadi

ABSTRACT

The growth of the world's population leads to increased energy needs. The use of fossil energy leads to challenges. The main reason for this is that the use of fossil fuels has a negative impact on global climate change, and the world is heading towards running out of fossil fuels in a few years. Renewable energy sources like photovoltaic and wind power plants are good solutions for those challenges. For the generation of clean energy, batteries are not necessary. Most renewable energy sources are intermittent in nature, which is why battery energy storage systems could be useful.

There are mainly two types of converters for converting direct current to alternating current. They are voltage-source inverters and current source inverters. A voltage source inverter is well-known and widely used in many industrial applications. But a little research has been done about current source inverters due to some problems such as open circuits and large inductances on the DC side.

The project deals with the Current Source Inverter for Battery Energy Storage System. The main objective of this project is to model, design, control, and simulation a current source inverter and analyse the advantages and disadvantages of both converters, with focus on the current source inverter.

In this thesis, a cascaded control structure is used for controlling three-phase grid-connected CSI. Current and voltage control design and simulation of CSI will be the focus. The proportional integral controller (PI-controller) is used to control the inverter. To verify the theoretical study, a simulation model in MATLAB/Simulink is built and verified.

Keywords

Current source inverter, voltage source inverter, battery energy storage system, pulse-width modulation, proportional integral control and grid-connected.

Contents

List of Figures

List of Tables

Abbreviations

CSI	Current source inverter
VSI	Voltage source inverter
BESS	Battery energy storage system
PI-control	Proportional integral control
AC	Alternating current
DC	Direct current
PWM	Pulse width modulation
SVM	Space vector modulation
PLL	Phase locked loop
dq0	Direct-quadrature zero
CCS	Carbon capture and storage
CO_2	Carbon dioxide
IGBT	Insulated-gate bipolar transistor
MPPT	Maximum power point tracking
IEEE	Institute of electrical and electronics
IEC	International electrotechnical commission
THD	Total harmonic distortion
RMS	Root-mean-square (of instantaneous current/voltage values)
FET	Field-effect transistors
BJT	Bipolar junction transistors
MOSFET	Metal-oxide-semiconductor field-effect transistor
f_{sw}	Switching frequency
PV	Photovoltaics
VSD	Variable speed drive
RPM	Revolutions per minute

Chapter 1

1 INTRODUCTION

1.1 Background

The rapid increase in the world's population will require more and more energy generation. A carbon footprint is created when energy is produced using fossil fuels like coal, gas, and oil. Furthermore, fossil energy sources are not sustainable energy sources, which means non-renewable energy sources are limited, and increasing population leads to increased usage of them. Therefore, new solutions must be in place; otherwise, soon, there will be a lack of fossil fuel [1]. The nuclear plants are debatable to be safe anymore after a couple of incidents, and the nuclear waste storage is an unsolved issue [2] [3]. Another huge risk is global warming. The situation is getting worse and worse each year, which is why events such as United Nations climate change conferences are organized. The Paris Agreement, or COP21 conference, was held in 2015 in the French capital. 195 countries were participating, and most of those countries signed an agreement to reduce greenhouse gases and keep the global warming temperature well below 2 °C (pre-industrial levels).

This requires substantial CO_2 emissions reductions compared with the baseline, the New Policies Scenario. As figure 1.1 illustrates, energy efficiency and the integration of renewable energy sources are expected to account for 80% of the CO_2 emission reductions by 2040. This conference directed a new point of view in energy production, transformation, transmission, and even usage. The production will be achieved by using renewable energy sources such as wind parks, solar systems, hydro plants, biomass, geothermal energy, etc. [4]. As shown in the figure below, DC-to-AC power converters play an important role in the New Policies scenario; indeed, DC-to-AC power converters can contribute to the use of renewable energy and make renewable energy more efficient.

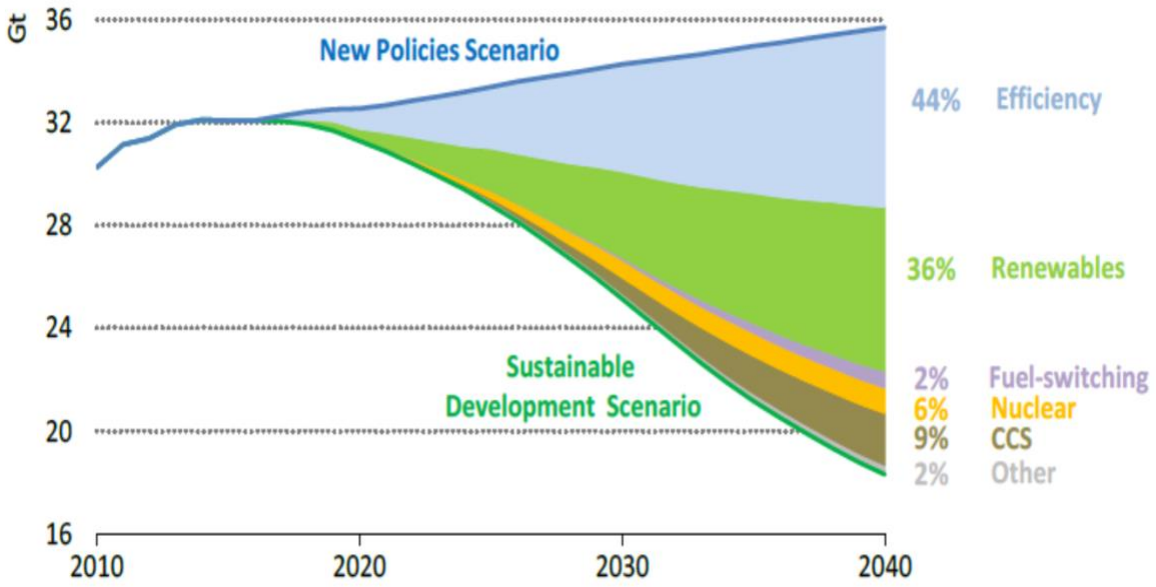

Figure 1.1-Global CO_2 emissions reductions in the New Policies and the Sustainable Development Scenarios [5].

One of the most challenging problems in using renewable energy sources is energy storage. Because photovoltaics (PV) and wind output are not constant all the time, we need some storage system that can provide backup at any time. Therefore, energy storage systems play a vital role in the electrical power system, and the development and advancement of power electronics technologies and various energy storage technologies will be beneficial for increasing the efficiency of the power system. It is not easy to store the electricity in large quantities, but we can convert the energy into different forms and store it, such as electrochemical, electromagnetic, kinetic, and potential energy. Based on these forms, some energy storage technologies have been developed, and some are under development. Figure 1.2 shows the percentage of energy storage systems with installed capacity worldwide. Some energy storage technologies are as follows:

- Compressed air energy storage
- Flywheel
- Super capacitor
- Battery
- Pumped hydro (storage)
- Super conducting magnetic energy storage

The oldest form of energy storage is battery storage, and the currently available battery technologies are based on flow battery technologies or conventional battery technologies. The world's largest lead acid battery energy storage system, rated at 40 MWh, was installed in California, USA [6]. Battery storage systems are relevant for this project.

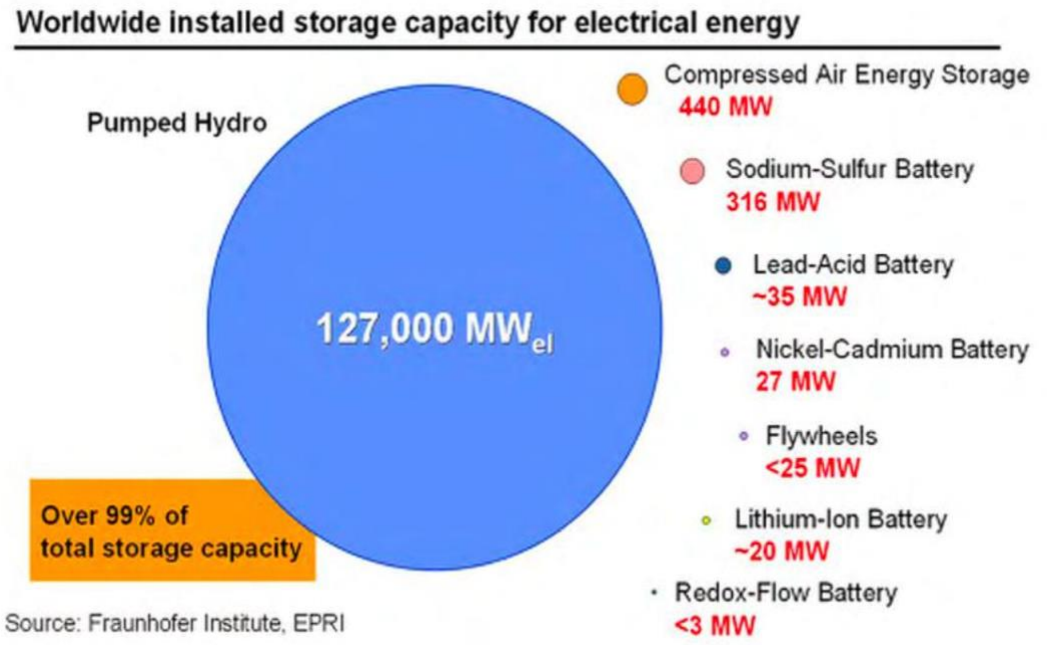

Figure 1.2 Energy storage systems is installed capacity worldwide [7].

The DC to AC power converter is categorized into two types: voltage source inverters (VSI) and current source inverters (CSI). They can be categorized into various topologies, like three-phase, single-phase, and multilevel switching arrangements, depending on the voltage and rated power requirements of the dedicated application. From the perspective of photovoltaic systems and wind turbines in multimegawatt ranges, CSI topology seems to be a better choice as compared to its competitor, VSI [8–9]. A lot of research has been done on VSI, which is widely used in many industrial applications. But VSI has some drawbacks, such as the current shoot-through problem [10] and the need for a step-up transformer.

Although CSI has attracted less research attention than VSI since it has some drawbacks like an open-circuit problem and must have a large inductance on the DC side, CSI may become a direct competitor of VSI. CSI has several advantages, such as inherent short-circuit protection and the fact that inductors have a much longer lifetime as compared to electrolytic capacitors. There are several types of modulation techniques that can be used to control the CSI, such as space vector modulation (SVP) and carrier-based sinusoidal pulse-width modulation (CSPWM). In this project, direct duty-ratio PWM (DDPWM) modulation techniques and PI-control in the direct-quadrature zero (dq0) frame are used to control and analyse of the three phase CSI in grid-connected mode.

1.2 Objective of the work and motivation

The world is facing an energy crisis, and everywhere people are focusing on renewable energy systems and working on the integration of battery storage systems with grid-connected converters. Renewable energy systems are the future of electric power generation. This being the case, both graduate and undergraduate studies of electric power should provide practical knowledge about the architecture of solar PV power generation systems. CSI could potentially address some of the above issues and is therefore worth researching more about. Traditionally,

CSIs have found little usage in industry in general due to their simplicity in terms of current control [11]. The main objective of the project is to study, control, test, and create a MATLAB/Simulink model of CSI. The goal of this thesis is the following:

- Review of relevant literature.
- Review of different inverter types.
- Study about working of three phase CSI and BESS.
- Modelling and simulation of DC-AC inverter and its control.
- Design and MATLAB/Simulink simulation model of CSI based on BESS with focus on power electronics and control.
- Comparative analyses between CSI and VSI based on BESS including total harmonic distortion, efficiency, dynamic response, bidirectional power flow.

1.3 Structure of the report

This thesis is structured with sections enumerated as X.Y.Z.A., where X is the number of the chapter, Y is the number of the section, Z is the number of the subsection, and A is the number of the subsubsection within the chapter X. Tables and figures are expressed as X: Y, where X is the number of the chapter and Y is the number of the figure or table in chapter X. The equations in this project are expressed in the form (X.Y), where X is the number of the chapter and Y is the number of the equation in chapter X. References are cited in the text with square brackets as [X], where X is the number of references, and are listed according to the Institute of Electrical and Electronics Engineers (IEEE) citation style.

Chapter 1 [1 Introduction]

This chapter briefly represents the general goal of the project, the need for renewable energy sources, the storage of energy, and the DC-AC power converter. The next subsection represents the objective of the work and its motivation.

Chapter 2 [2 Current source inverters versus voltage source inverters, and battery energy storage system]

This chapter briefly compares the two-power converters, namely CSI and VSI. In this chapter, we will discuss and describe some of the advantages and disadvantages of both CSI and VSI. This includes such things as: boosting capability, inherent short-circuit immunity, efficiency, complexity of the control system, and BESS (which includes a description of different types of batteries and a more detailed description of some types).

Chapter 3 [3 Description and modelling of current source inverter]

Chapter 3 describes CSI theoretically, the working principle of three phase CSI, CSI topologies, harmonics in CSI, and different AC filter types.

Chapter 4 [4 Control strategy of the current source inverter]

Chapter 4 represents a comprehensive discussion about the control strategy of the CSI. This includes the choice of control type, controller optimization signal reference frames, cascade control, PI-control, tuning methods for PI-control, PWM, and a mathematical model for the control system of the CSI in grid-mode.

Chapter 5 [5 Simulation and discussions of result]

This chapter provides a discussion about the simulation and the results obtained from the simulation process. A CSI with its control system and DC voltage source is implemented in a MATLAB/Simulink model and tested to analyse the functionality of the control as well as the voltage and current output.

Chapter 6 [6 Conclusion and future work]

The last chapter represents the concluding remarks from the thesis and the proposals for further work.

Chapter 2

2 Current source inverters versus voltage source inverters, and Battery energy storage system

An inverter is the heart of an electrical power generation system. The inverter plays a key role in power electronics devices, and their safety and reliability are important indicators for evaluating those devices. As mentioned earlier, the power converter is very important to convert DC-current to AC-current at the desired output voltage and frequency, also fundamental to reduce greenhouse gas emissions and contribute to more sustainable and efficient mobility [12]. Inverters can be classified into two types, VSI and CSI, based on their input sources. Most researchers mainly focus on VSI, which is widely used in the industry, there are some advantages and disadvantages to both CSI and VSI.

2.1 Voltage source inverter

VCI consists of six semiconductor switches with gate-turn-off control and their associated freewheel diode, usually incorporated within the device package in modern devices. The six devices create three separate phase legs (a, b, and c) within the inverter, with the canter point of each leg being a connection point for the load being driven. Figure 2.1 shows the topology of a three phase VSI system: there are six fully controlled switches from S1 to S6, and two IGBTs relate to each phase of the source. The IGBT connected in one lag does not turn on at the same time; if we do so, a short circuit occurs between the positive and negative sources, just as S1 and S2 or S3 and S4 cannot be turned on at the same time.

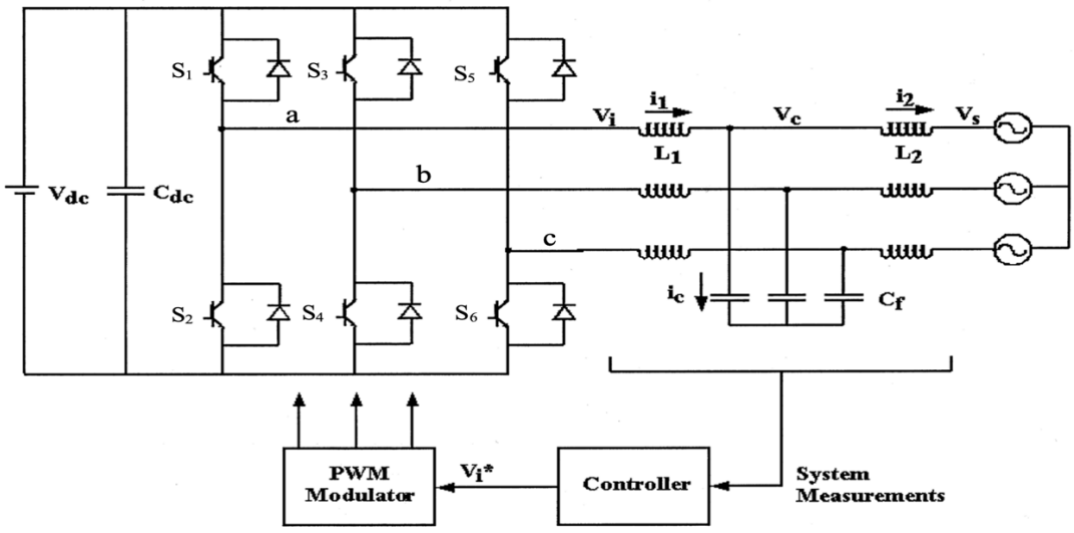

Figure 2.1 Topology of three phase VSI system [13].

2.1.1 Six-Step Switching

A six-step operation involves switching at the frequency of the inverter output. For example, each switch turns on and off once during output period 2 and has an "on" duration of radians. Each phase leg is offset by radians, creating six equal intervals (I to VI) during one output period. The switching order is the number order of the switches and results in there always being one switch from each leg conducting, except for a small time to allow the conducting switch to turn off before the switch from the same leg is turned on. The delay period is known as the blanking time and is required to prevent both switches within a leg from conducting simultaneously, shorting the DC link, and causing a shoot-through fault, where current rises rapidly and is likely to cause the device(s) with the inverter to fail. V_{an}, referenced to the load star point. Voltage control in a six-step system is only achievable by varying the DC link voltage unless multiple inverters are used. Control of the DC link voltage depends on the source of the DC, this can be achieved with a DC chopper when used with a DC source (such as a battery), an uncontrolled rectifier with an AC source, or by using a controlled rectifier from an AC source [14].

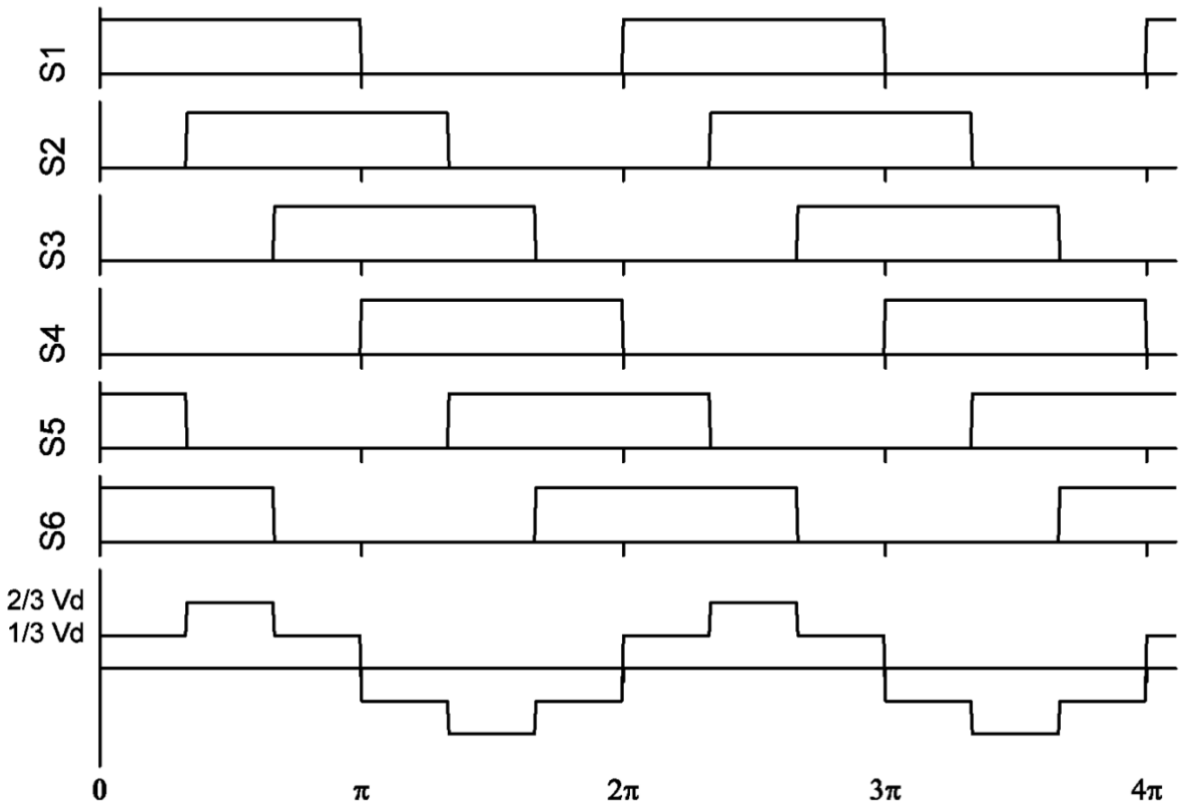

Figure 2.2 VSI six-step switching [14].

2.1.2 Advantages of voltage source inverter

A lot of investigation has been done about VSI for the past decade. And the VSI is the most used converter today because it has some features. The output voltage of VSI is constant at any load condition. VSI has higher efficiency; therefore, it does not require any series reactors. VSI has an easier control mechanism and a relatively small harmonic. VSI can operate steadily with open-loop V/HZ control [15]. Moreover, nowadays VSI design is fully integrated into a chip, which has higher reliability, faster dynamic response, low cost, and minimizes the install time [16].

2.1.3 Disadvantages of voltage source inverter

VSI is a boost-type converter; the output voltage assumes a wide range of values but is always greater than the maximum instantaneous value of the phase-to-phase power grid voltage. Therefore, it is necessary to use a dc-dc back-end buck-type converter to adjust the dc-link voltage to a level appropriate to charge the batteries (typically, the nominal voltage in the batteries is below 560 V, which is the maximum instantaneous value of the phase-to-phase voltage). This is one of the drawbacks of this converter compared with the CSI. Also, VSI always required a dc-dc boost converter for boosting and regulating its input voltage. By adding a converter stage, it requires two individual control systems, which leads to a more complicated control scheme and reduces the reliability and efficiency of the overall system [17].

2.1.3.1 Electrolytic Capacitors

The input side of a VSI is a voltage source; a large capacitor is used for this purpose. The polarity of the input voltage does not change, and therefore the direction of power flow is determined by the DC current input. And the large, usually electrolytic, capacitor at the heart of a VSI can potentially cause problems if the inverter is used in certain environments. The capacitors are generally packaged in a sealed aluminium can, which, when subjected to low atmospheric air pressures (typical of flying at altitude), as is the case in aircraft, can become distorted, usually causing catastrophic failure. Existing solutions involve sealing or maintaining the atmosphere around the capacitor at ground level or removing it completely from the system [14].

2.1.3.2 Start-up and Shutdown

When energizing a variable speed drive system (VSD), consideration of the possible inrush current is required to ensure the correct start-up of the system. The large, electrolytic capacitor present on the DC link will begin charging as soon as a DC voltage is applied. If the supply is not controlled or current limited, the low impedance of the capacitor will result in a current surge during the initial start-up. This surge will be severe, possibly damaging other components. The susceptible components include the input rectifier in an AC: DC:AC system, the capacitor itself, and protection devices on the supply side of the VSD. Operation of supply fuses, or circuit breakers, to interrupt inrush current is a nuisance trip that should be avoided, since the owner/operator of the drive system will tend to incorporate higher rated and hence less effective protection devices [15]. Some other drawbacks of VSI are that it is basically a bidirectional converter and cannot convert AC power to DC power. Moreover, VSI has a current shoot-through problem [18].

2.2 Advantages of current source inverter

Even though most research works focused on and studied the VSI, CSI also has its own unique characteristics that the VSI does not. More and more benefits of CSI can be discovered if CSI gets more attention from researchers. This led to the CSI being used in more different devices, making it a real competitor to the VSI. Some research has been done on CSI, which can be categorized into several groups: hybrid topology machine control applications, non-machine applications, CSI machine control applications, and so on. Here are some advantages of the CSI:

2.2.1 Inherent Short-circuit Immunity

One of the main benefits of CSI is that a short-circuit of a phase-leg (an upper and a lower switch at one phase-leg can be turned on) will not cause a short-circuit current both on the DC-side and on the AC-side. Due to the presence of a relatively large inductor connected in series with the input power source. On the AC-side, since the semiconductor components can conduct current in one direction only (switches are reverse-blocking), a short-circuit is not possible unless the semiconductors are damaged. On the DC-side, during a short-circuit of a phase-leg, the DC-link inductor would impede the sudden rise until its saturation [19].

2.2.2 Boosting capability

Three-phase CSI has boosting capability on its fundamental output through its DC-link inductor, which acts in the same way as a DC-DC boost converter. Advantage of its implicit voltage-boost characteristic to provide continuous interconnection between the low and variable dc voltage and the high fixed AC grid voltage. This is the reason why a DC-DC converter is unnecessary [20]. Moreover, the voltage boost function can be used in their application as a fuel cell-to AC interface. Fuel cells have poor voltage regulation at full load [14]. In addition, boosting capability will reduce circuit and control complexity, reduce power losses, and increase the reliability and efficiency of the overall system.

2.2.3 Flux-weakening Control and Control of High-Speed Low Inductance Machines

The other benefit of CSI we can mention is flux-weakening control and control of high-speed, low inductance machines. Flux-weaking is a well-publicized method of controlling brushless machines to realize reduced torque, an extended speed operating region, and near constant power, as shown in Figure 2.3. The machine supply voltage and current constraints on traction characteristics are desirable in many applications, including automotive and marine traction, but also in aerospace, where activation of aircraft flight surfaces often requires such performance envelopes. Flux-weakening operation should allow for drive system design optimization, leading to improved utilization of the power supply, electronics, machine electro-magnetic, a reduction of the motor mass or volume of the machine, and/or the VA rating of the inverter components [14].

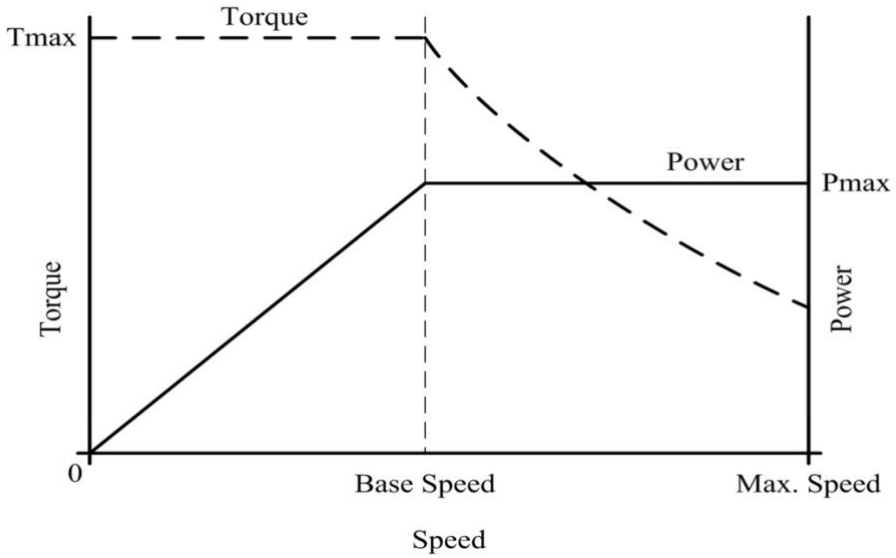

Figure 2.3 Typical traction torque-speed characteristic [14].

One consequence of designing a high performance, efficient high-speed (10's of 1000's of revolutions per minute (rpm)) parament magnet machine is that, in general, they have a phase inductance that is lower than a machine with a more typical (up to 3 Krpm) speed range. The cause of this low inductance can be attributed to many factors, but it generally arises from the design considerations for high speed. The low inductance machine will create control problems as the low impedance path that the inverter and motor present to the DC link capacitor will result in large current transitions but low average current levels if the PWM frequency is not high. Moreover, high PWM and current sensor sampling times make accurate control of the machine current difficult; the switching devices must also be rated sufficiently to operate reliably with the high peaks. Increasing the switching frequency could improve the performance of the machine, but the frequency will be limited by the device specifications and control system capabilities. This phenomenon will be exaggerated at low or zero speed, when the back-electromagnetic force is negligible. Poor control of phase current results in a greater phase current ripple, which will create torque ripples on the machine shaft, and induce additional machine losses. A CSI system can address the current control issues by utilizing the DC link inductance to limit the rate of change of the machine phase current, but this will influence the dynamic performance of the drive system [14].

2.3 Disadvantages of current source inverter

All devices have their own drawbacks, and CSI is no exception. One of the drawbacks of CSI is open-circuit faults [21]. But the immediate damage caused by open-circuit faults is minor and does not damage the devices like short-circuits in VSI. CSI also has lower efficiency than VSI in medium-voltage drive systems due to the DC-link inductor [22]. But CSI has a higher conduction loss and a lower switching loss than VSI, in total power loss, the efficiency differences between CSI and VSI are very small, and they can be improved [14].

2.3.1 Bidirectional Current source inverter

Conventional CSI is a reverse-voltage-blocking switch; in other words, conventional CSI is not a bidirectional converter like VSI. So, a conventional CSI cannot charge and discharge the

batteries, which is a drawback of CSI. But this problem can be solved, and it is fully possible to have a bidirectional CSI. DC/DC-boost converter is bidirectional since the system uses a regenerative brake [23].

The topology chosen in Figure 2.4 for the development of this application is based on the coupling of a CSI and DC/DC converter; these topologies are made up of silicon carbide devices and operate at high frequency activation, which reduces the size of the passive elements. Bidirectional CSI is described in more detail in this previous work [23].

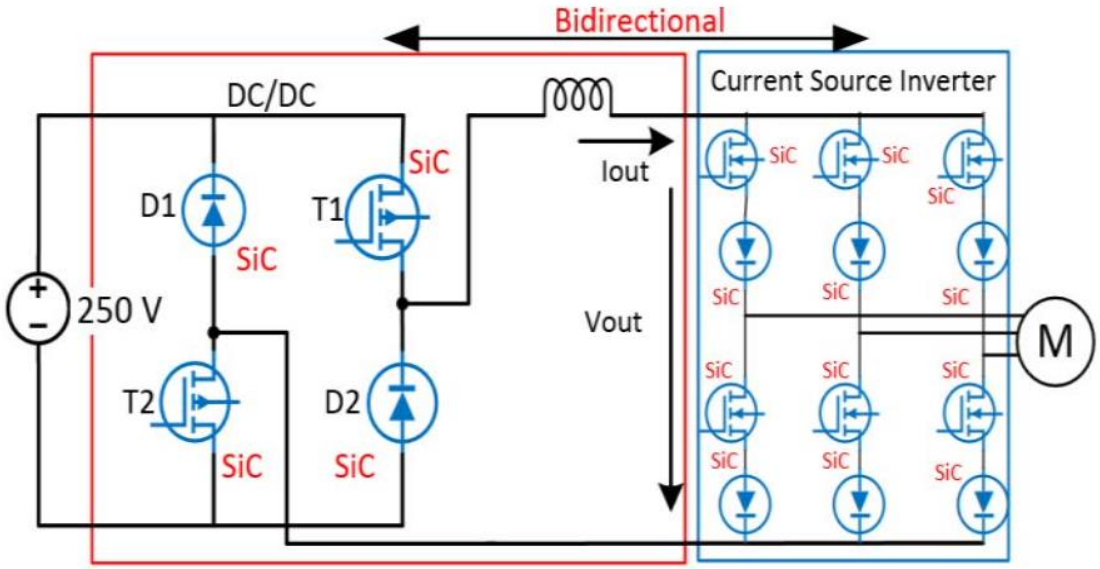

Figure 2.4 Topology CSI bidirectional [23].

2.4 Summary of CSI versus VSI

Both inverters have their own advantages and disadvantages, and both topologies can achieve the main target of an AC output to be injected into the grid (or in a standalone system) with controlled magnitude, phase, and frequency from a DC source. A comparative analysis of CSI and VSI is important to select the appropriate inverter based on the application, economic considerations, and its performance in varying environments. Finally, we can summarize the important differences between CSI and VSI in the table below.

Table 2.1 Comparison between the CSI and the VSI

Comparison criteria	CSI	VSI
DC-link	Constant current	Constant voltage
DC-storage	Inductor	Capacitor
Output-filter	CL	L/ LCL
AC-current	Direct controllable	Dependent on the load
AC-voltage	Dependent on the load	Direct controllable
Buck or boost type	Boost	Buck
Switching requirement	An overlap time	A dead time
Short-circuit protection	Simple	Necessary/Complex
Open-circuit protection	Necessary/Complex	Simple
Switch type	Reverse-blocking	Reverse-conducting
Switching loss	Low	High
Conduction loss	High	Low

2.5 Battery energy storage system

Renewable energy sources are the best solution to provide green energy to overcome global energy issues. And energy storage systems play a vital role in balancing the fluctuations in supply and meeting the ever-growing demand for electricity. For short-term requirements, battery storage can bring about frequency control and stability, and for longer-term requirements, it can bring about energy management or reserves. Storage is used to complement primary generation as it can be used to produce energy during off peak periods, and this energy can be stored as reserve power, as illustrated in Figure 2.5. The graph explains that system demand can be handled efficiently if storage is incorporated into the electrical network. As shown, the storage is charged from the baseload generating plant during the early hours of the day when demand is low. And then, as the demand rises during the day, the generating plants belonging to the mid-merit category account for the demand. And during peak demand, the peaking plant, which runs only for a few hours of the day, decreases the total cost of operating such a storage-incorporated system. Thus, we see that when the generation profile with storage is taken, there is a much-controlled demand graph as storage takes care of the load levelling, and then it is charged again at the end of the day from the baseload generating plant [24].

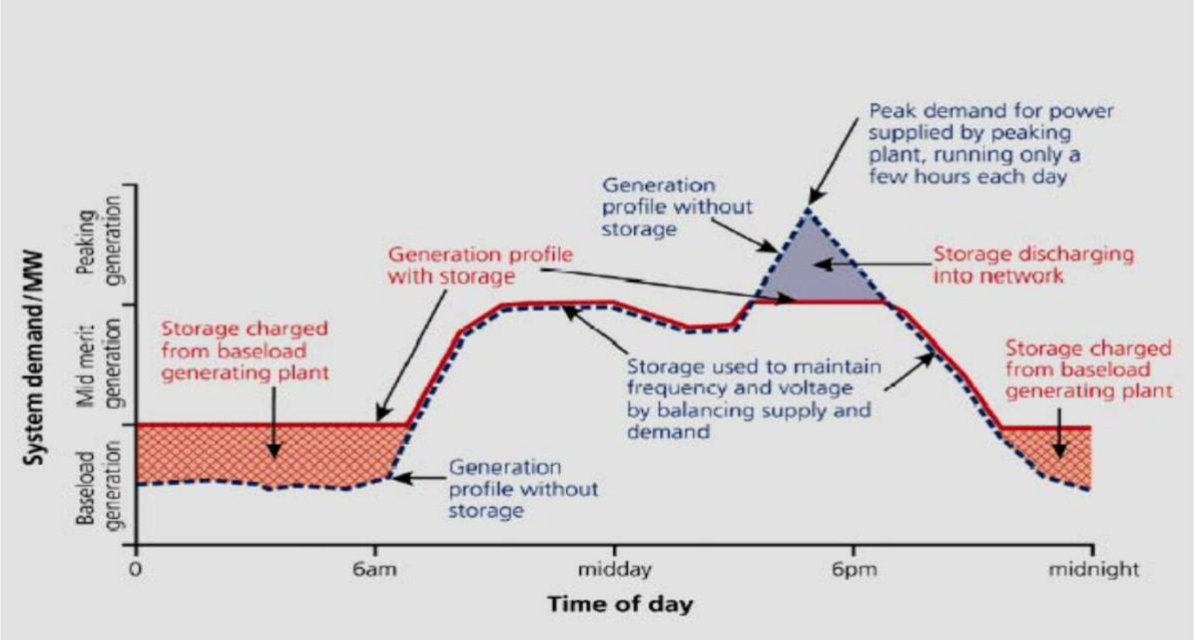

Figure 2.5 Charged storage and demand system [25].

Energy storage plays an important role in the electrical power system. The development and advancement of power electronics technologies and various energy storage technologies will be beneficial for increasing the efficiency of the power system. Here are some benefits of energy storage systems for the utility grid and power system:

- Energy storage can bring about a reduction in operating costs or capital expenditures when used as a generation resource in the utility sector.
- Energy storage can increase the usability of renewable energy resources such as PV and wind generated electricity by making this generation coincide with peak load demand. Energy storage may facilitate the inclusion of wind and solar energy into the power grid.
- Energy storage may increase the existing transmission and distribution equipment and eliminate the need for expensive transmission and distribution additions. Energy storage reduces the load on peaking transmission lines.
- Deferral of the construction of new transmission lines, transformers, capacitor banks, substations, or their subsequent upgrades. Transmission line stability, preventing a possible power system collapse. Increasing the power quality of the service would result in the protection of customer equipment.
- Energy storage is used in standalone applications, where it serves as an uninterruptible power supply unit. Uninterruptible power supply units are basically used for backup power, whereas energy storage can serve several online applications.

2.5.1 Battery operation principle

There are a wide variety of battery types serving various purposes. In a chemical battery, charging causes reactions in electrochemical compounds to store energy from a generator in a chemical form. Upon demand, reverse chemical reactions cause electricity to flow out of the

battery and back to the grid. Electric energy is released during discharge through a redox reaction. A basic battery cell consists of:

- The negative electrode, or anode, gives electrons and is oxidized during the redox reaction.
- The positive electrode, or cathode, accepts electrons and is reduced during the redox reaction.
- Electrolytes provide a medium for the transfer of electrons.

The two electrodes are interconnected with an external circuit, which allows charge and discharge of the cell. Depending on the desired output voltage and current, multiple cells can be connected in serial or parallel. There are several technologies to store electrical energy in batteries. The oldest, most classical, and mature technology is lead-acid. New technologies under development include sodium sulphur and lithium ion [26].

2.5.2 Types of batteries

We can basically classify the battery into two main models: primary and secondary. The primary batteries are "single use" and cannot be recharged. Dry cells and most alkaline batteries are primary batteries. The secondary batteries are rechargeable, which is relevant for this project. There are mainly four major battery technologies for rechargeable batteries.

1. Sodium sulphurs
2. Lithium-ion
3. Lead-acid
4. Flow batteries

2.5.2.1 Sodium sulphurs batteries

The sodium sulphur battery consists of a positive liquid sulphur electrode and a negative sodium electrode separated by an alumina ceramic electrolyte. When the battery is discharged, positive sodium ions flow through the electrolyte and electrons flow in the external circuit, producing around 2 volts. This process is reversed during charging; the positive sodium ions pass back through the electrolyte and reform elemental sodium. The operational temperature of a sodium sulphur battery is high, 300 C. The high temperature is required to maintain the molten states of the electrodes. The efficiency is about 80%. A typical system has a rated power of 30 MW and can provide power for 6 hours. There are about 316 MW installed worldwide [27].

2.5.2.2 Lithium-ion batteries

Lithium-ion batteries consist of a litigated metal oxide cathode and a graphite carbon anode. The electrolyte is made up of lithium salts. During charging, lithium-ion from the cathode flow through the electrolyte, to the anode, where they combine with external electrons and are deposited as lithium atoms between the carbon layers. When the battery is discharged, this process is reversed. The efficiency of lithium-ion battery systems is high, about 90–95%. A typical system has a rated power of 1–10 MW [27].

2.5.2.3 Lead-acid batteries

Lead-acid batteries come in many variants, but all can be described by the same chemistry. The anode is made of lead dioxide, and the cathode is made of metallic lead. The electrolyte consists of sulphuric acid, which is consumed during the discharge. The efficiency of a lead-acid battery system is about 70–80%. A lead-acid battery system is the oldest and most recognized electrical energy storage system today in small to medium-scale systems. It has been the default choice for many small and medium scale energy storage applications despite many disadvantages such as low life exaptation, low energy density, high maintenance, and environmental hazards related to the handling of lead and sulphuric acid. Lead-acid battery systems can be used in different applications, and the technology has been used in large-scale energy management applications [28]. As mentioned before, the world's largest lead acid battery energy storage system installation was a 10 MW, 40 MWh system in California, USA, and its operational period was 1988–1997.

2.5.2.4 Flow batteries

The flow battery energy storage system consists of two sets of electrolytes that flow through two independent loops. The loops are joined in the cell but separated by a membrane that prevents the electrolytes from mixing but allows ion-exchange. Flow batteries are easier to scale than conventional battery cells. In fact, when the electrolytes are stored outside the cell, it is possible to increase the energy storage capacity simply by increasing the volume of the electrolyte reservoirs. This makes the technology suitable for large-scale systems. The amount of energy stored is determined by the size of the tanks. The flow battery has about 75% efficiency [24].

Chapter 3

3 Description and modelling of the current source inverter

Characteristics of CSI include a simple converter structure and inherent voltage boost capability. CSI provides a low instantaneous rate of voltage change with respect to time in comparison to VSI and multilevel inverters. The input side (DC side) of CSI is a current source. An inductor is connected at the input side of CSIs to maintain the current [29]. The polarity of the input current does not change, and the direction of power is determined by the input voltage. In the output, CSI generates an alternating current wave with a fixed magnitude (for a given input) and adjustable time.

3.1 Current source inverter topologies

The distributed generation system of CSI can be classified into two categories: grid-connected and standalone (feeding local loads). In grid-connected systems, the energy stored can be directly converted to AC-power and transferred to the grid. To achieve this, the inverter must be controlled in a pre-defined way using control loops so that maximum power can be transferred to the grid. The output terminals of inverters cannot be directly connected to the grid due to harmonics. A filter is used to negate this effect. In a standalone system, storage batteries are used to store the energy obtained from these intermittent sources. These batteries serve as input to the inverter, which converts DC power into AC power. There are different levels of CSI, such as multilevel CSI and n-level CSI. [30]. Figure 3.1 shows the generic n-level CSI structure. There are two main types of CSI in general: three-phase and single-phase CSI.

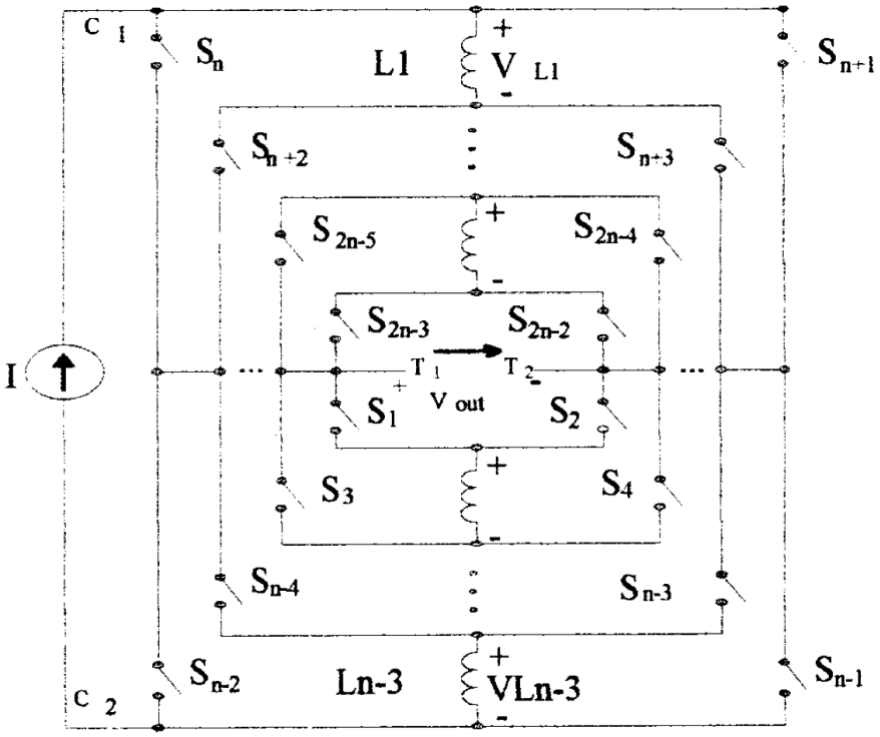

Figure 3.1 The generic n-level CSI structure [30].

3.1.1 Single phase Current source inverter

The CSI can be divided into two main types: three-phase and single-phase. A single-phase CSI has a simple operation process, and it is easier to control a single-phase CSI than a three-phase CSI. A single-phase current source inverter has four IGBT switches and four diodes, assigned as (S1, S2, S3 & S4). Each diode is connected in series with an IGBT switch for reverse voltage blocking capability. A single-phase system has even harmonics on the DC-side, which affect maximum power point tracking (MPPT), reduce PV cell lifetime, and are associated with odd-order harmonics on the side. Therefore, eliminating the even harmonics on the DC-side is essential when a single-phase CSI is used [31]. A schematic diagram of single-phase CSI is shown in Figure 3.2.

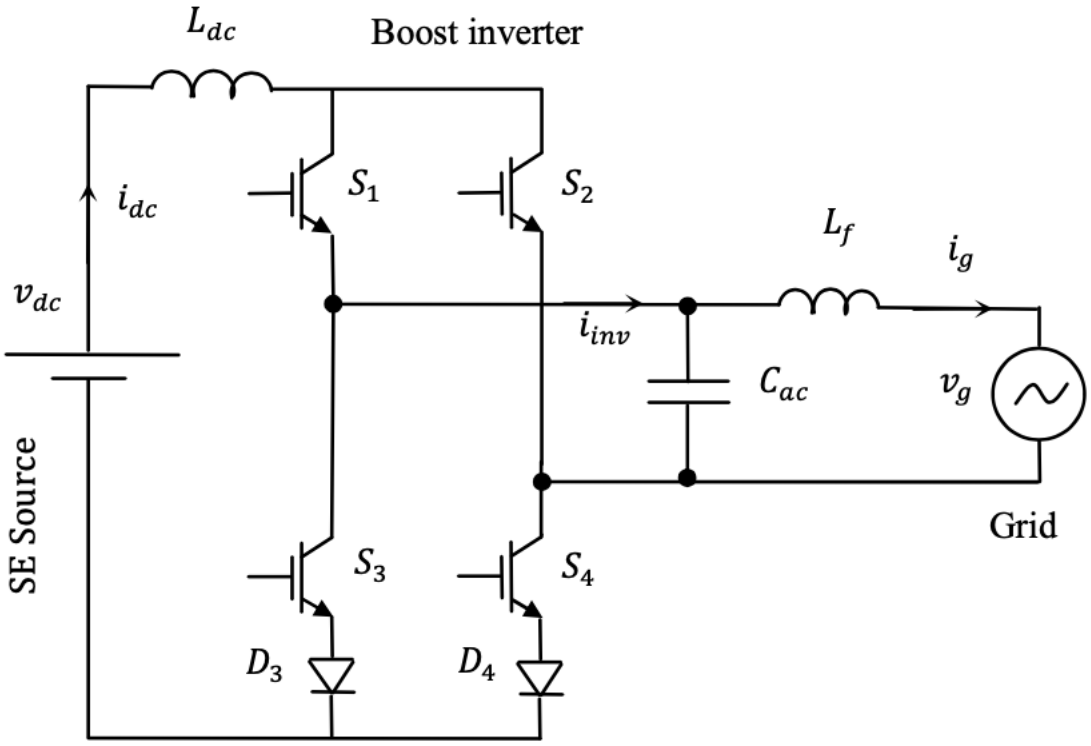

Figure 3.2 Circuit diagram of single-phase CSI circuit [32].

3.2 Working principle of three phase current source inverter.

The three-phase CSI has nine possible switch combinations, of which six are self-commutated unidirectional switches with active space vectors and three are zero space vectors. CSI has six insulated-gate bipolar transistors (IGBT) and six diodes placed in series with the IGBTs, as Figure 3.4 illustrates. The diodes placed in series with the IGBTs are necessary since, during the normal operation of the inverter, the power switches must withstand the direct and reverse voltages (u_{Idc} and - u_{Idc}) produced by the DC inductor. The angles between space vectors are 60°. Figure 3.3 illustrated Space-vector state for both active and zero switches. The space vectors of the current in CSI are: i_{0a}, i_{0b} and i_{0c}. It can be defined as follows:

$$i_0 = i_{0a} + i_{0b}e^{2j\pi/3} + i_{0b}e^{4j\pi/3} \qquad (3.1)$$

Where:

i_{0a}, i_{0b} and i_{0c} are the line currents on output side of CSI.

The switches experience bipolar voltage stresses, with the maximum peak voltage equal to that of the AC voltage.

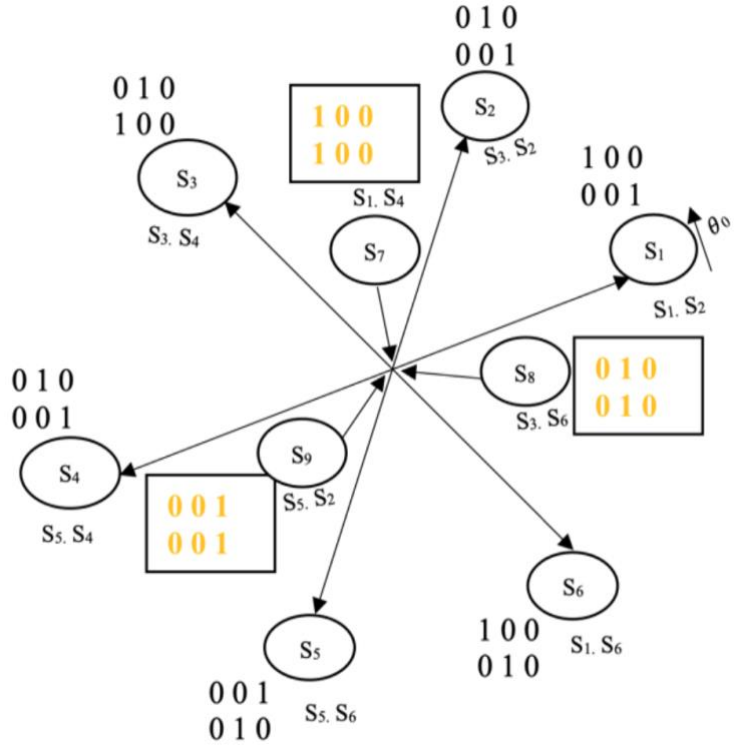

Figure 3.3 Space-vector state for three-phase CSI.

An inductor on the DC-side of CSI is an energy storage device for CSI. The filter capacitor on the inverter's AC side is used to attenuate high frequency harmonics depending on the modulation switching frequency (f_{sw}). CSI in Figure 3.4 generates three-level current output levels: i_{dc} and 0. One switch from the upper group and one from the lower group (S1, S3, S5 & S4, S6, S2) must be on for each instant. For the six active states of the current source bridge; in each one the DC-link current is output from one leg and drawn from another one. The output current is zero when both switching devices are turned on in the phase leg. The three-phase CSI does not contain even harmonics at the DC side or 3rd harmonics at the AC side of the system. In an islanding mode of operation, CSI behaves as a static synchronous generator that sets the AC frequency and gradually builds up its output voltage from 0 to the rated voltage. It then establishes a stiff AC bus, where the load is connected [33].

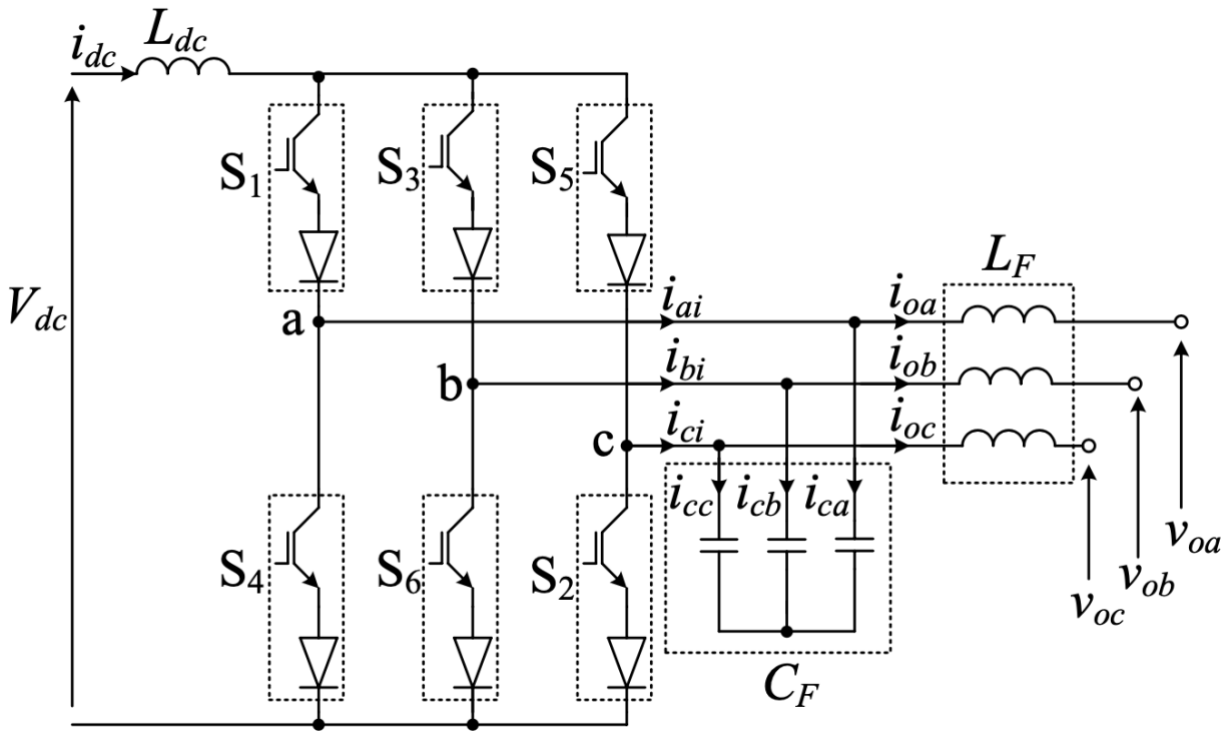

Figure 3.4 Circuit diagram of a three-phase CSI circuit [34].

3.2.1 Transistor

On a broader scale, the transistor can be classified into three major types: IGBTs, field-effect transistors (FETs), and bipolar junction transistors (BJTs). Alle type transistors basically consist of two PN (p = polarity of the emitter terminal & polarity of the base terminal) diodes connected back-to-back. It has three tree terminals, namely the emitter, base (gate), and collector. The basic idea behind a transistor is that it lets you control the flow of current that's flowing through a second channel.

An IGBT is a three-terminal device (a power semiconductor) that is used as an electronic switch and has high efficiency and fast switching. IGBT is a semiconductor device with four alternating layers (P-N-P-N) controlled by a metal-oxide semiconductor gate structure. In Figure 3.5 is shown the operation of IGBT. IGBT is designed to turn on and off rapidly and is used in high switching applications. IGBTs are mostly used in variable frequency drives where quick switching is required. It allows power to flow in the on state and stops it when it is in the off state. IGBT is a unidirectional device; it can only switch current in one direction, which is from collector to emitter (forward), unlike metal-oxide-semiconductor field-effect transistor (MOSFET), which can switch current in both directions (forward and backward) [35].

MOSFETs are commonly used in impulse power supplies with operating frequencies above 200 kHz and in charging devices for accumulative batteries. The main criteria for selecting transistors are operating current and voltage. The choice of the transistor should be made with a margin of voltage to prevent its failure; therefore, an IGBT has been chosen for this project. The IGBT has the following characteristics:

- Small losses in the open state at high currents and stresses.
- Switching characteristics and conductivity are identical to those of a bipolar transistor.

- IGBTs are controlled by voltage.
- IGBTs are used for voltages greater than 1000 v, high temperatures (above 100 °C), and high output power (more than 5 KW).
- IGBTs are used in motor control circuits (with an operating frequency of less than 20 kHz), uninterruptible power supplies, and welding machines.

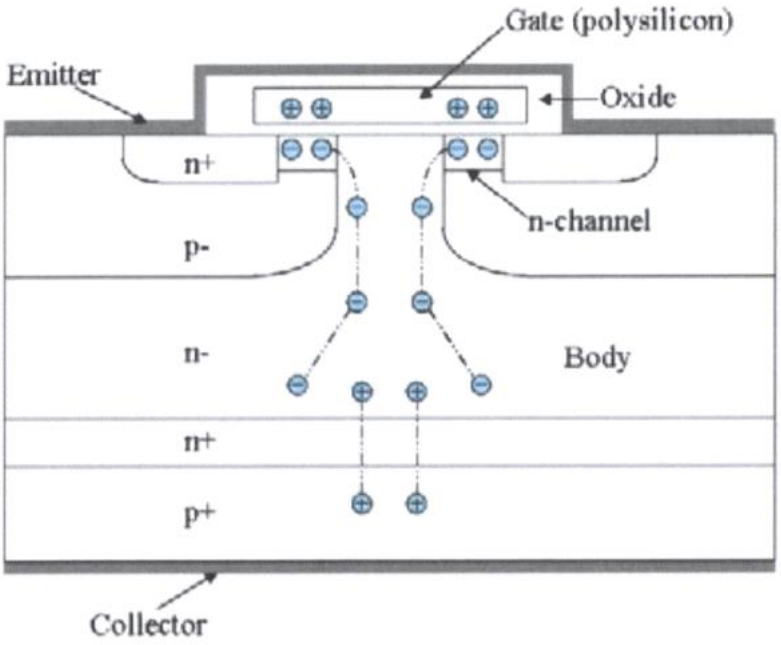

Figure 3.5 Diagram for IGBT Operation [35].

3.2.2 Diodes

Diodes consist of two electrode elements whose conductivity depends on the direction of the current flow. The most common function of a diode is to allow an electric current to pass in one direction (called the diode's forward direction), while blocking it in the opposite direction (the reverse direction). The diode is opened when a forward voltage is applied to it. The diode has a small resistance, and through it flows direct current. In this case, when the reverse voltage is applied to the diode, it is closed. This means that the reverse current is small, and in many cases, it is even zero. It is necessary to have both diodes and IGBT in the inverter because diodes make it possible for current to pass if it is needed. Diodes protect transistors against overvoltage's, which might destroy inverters.

3.3 Current source inverter in grid-connected

Integrating a distributed power system into an electric grid network has a list of requirements that need to be met to ensure a safe connection to the grid. Research based on the rules and regulations is necessary for the design of an approved grid connected active converter. The standards applied for interconnections between distributed power systems and the electrical grid varies around the world. Some nations and regions develop their own standards for the local grid utilities and for different voltage levels. Many countries have similar standards, which are mainly based on two major international standards from IEEE and the International

Electrotechnical Commission (IEC). The main and most vital requirements and limitations can be found in the standards provided by IEEE and IEC. The most relevant standard that compiles all technical requirements and tests for grid-connected distributed generation and operation can be founded in [36]. Some important requirements for the grid-connected inverter include:

- Low total harmonic distortion of the current injected into the grid
- Controlled power injected into the grid
- Maximum power point tracking
- High efficiency

The performance of the inverters connected to the grid depends mainly on the control scheme applied.

3.3 Harmonics in current source inverter

Inverters are switching devices that cannot be directly connected to the grid. Because the inverter produces harmonics, which degrade power quality. There are different standards in place [37–38], which put limitations on the harmonics that can be injected into the grid. The transformer's windings serve as inductance, which reduces the harmonics present in the current wave. may be used to connect the system to the grid [39]. Transformers are expensive and bulky, which makes the system costly. Therefore, it becomes more common to use a filter circuit as the interface in a transformer to connect an inverter to the grid. The sources of current harmonics are nonlinear loads connected to the distribution network. The flow of current harmonics through a network, which has a certain impedance, leads to the appearance of harmonic voltages and, accordingly, to distortion of the form of the supply voltage. Different types of loads and their curves are shown in figure below.

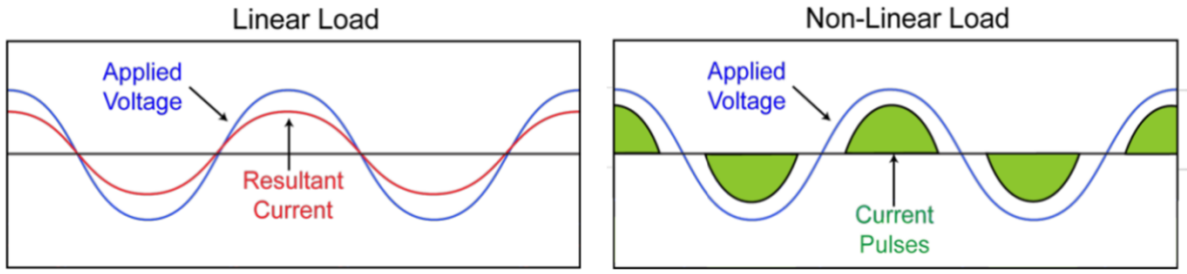

Figure 3.6 Voltage and current curves from the source by linear and non-linear loads [40].

Harmonics in the electrical signals (voltage and current) cause the decline of electric power quality. Harmonic can cause the following negative influences:

- Overload in distribution networks due to an increase of the current value.
- Overload in zero conductors due to the summation of higher harmonics currents, which are multiple of 3 and are generated by single-phase loads overload.
- Overloads, vibration and aging of generators, transformers, and electrical motors.
- Overloading in the distribution network can lead to higher levels of energy consumption and lossless increase.
- Distortion of the current curve shape can cause false triggering of circuit breakers which may lead to the shutdown of the production process.

Total harmonic distortion (THD) is a measurement of declination caused by harmonics. The THD is shown in percentage according to the size of the curve's change: the lower the percentage, the more a curve looks like an ideal sinus curve. The first harmonic is also called the "basic or fundamental harmonic; for a normal network in Europe, it is a 50 Hz harmonic. THD is mainly used to measure the distortion of the shape of the input or output current and voltage.

$$THD_U = \frac{\sqrt{U_2^2 + U_3^2 + U_4^2 + I + U_n^2}}{U_1} \qquad (3.2)$$

Where: U_2, U_3 …U_n are the R.M.S voltages of the n-th harmonic, and U_1 is the RMS voltage by fundamental frequency.

$$THD_I = \frac{\sqrt{I_2^2 + I_3^2 + I_4^2 + I + I_n^2}}{I_1} \qquad (3.3)$$

Where: I_2, I_3 …I_n are the RMS current of the n-th harmonic, and I_1 is the RMS Current by fundamental frequency.

Some typical values of THD are the following:

- 0% the waveform is an ideal sinusoid.
- 3% waveform is different from the sinusoidal, but distortion is invisible to the eye.
- 5% deviation of the waveform from sinusoidal is visible on an oscillogram.
- 10% standard level of distortion.
- 12% perfectly symmetrical triangular signal.
- 22% A "typical" signal of a trapezoidal or stepped form.
- 48% perfectly symmetrical square wave.
- 80% ideal sawtooth signal.

3.3.1 AC Filter

Pulse width modulation (PWM) switching causes high-frequency harmonics in the line current. The harmonic content is attenuated by the output low-pass filter. Inductive (L) filters are very common in VSI [41]. Other common filter configurations for VSI are inductive-capacitive (LC) and inductive-capacitive-inductive (LCL) filters. But in CSI, the most common topology filter is the second-order low-pass capacitive-inductive (CL) filter, as shown in Figure 3.8c. CL-

filters are used in CSI, because they attenuate high frequencies at 40 dB/decade [42]. The point of a grid-connected inverter is to supply good quality (low THD) power to the grid and meet the requirements in the standards as mentioned before [37-38]. The low-pass filter dirtiness causes harmonic suppression and influences the inverter power factor as well. The filter has iron and copper losses, which decrease the overall converter efficiency. The primary aim of the low-pass filter design is for the grid-connected converter to comply with the specified grid requirements [43].

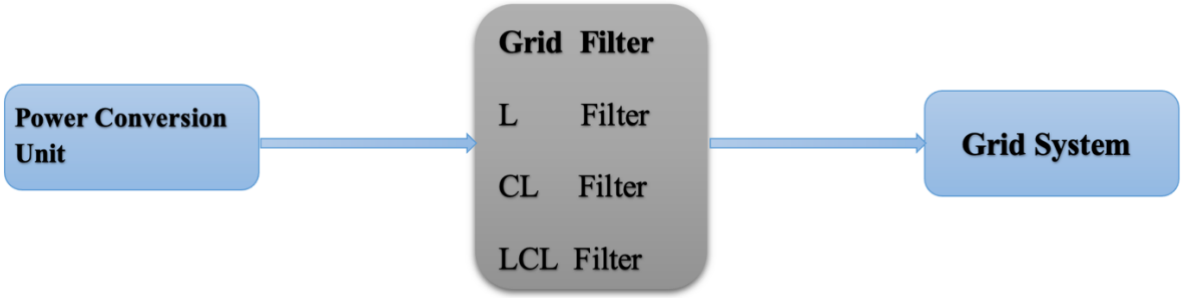

Figure 3.7 Grid filter interconnection with a grid-connected converter.

The filter cut-off frequency f_c is commonly referred to as the resonant frequency f_r, as the filter has an infinite gain at that frequency if there is no damping resistance. The output filter must be accurately damped to avoid any large amplification at the resonant frequency. The resonant frequency equation is as following:

$$f_r = \frac{1}{2\pi\sqrt{LC}} \qquad (3.4)$$

A quality factor Q is the inverse of damping, and it is related to the filter gain at the resonant frequency. The quality factor can be given by:

$$Q = \sqrt{\left(\left(\frac{R_D}{\sqrt{L/C}}\right)^2 + 1\right)} \qquad (3.5)$$

Where are:

f_r Resonant frequency
L Inductance of inductor
C Capacitance of capacitor
Q Quality factor
R_D Damping resistor

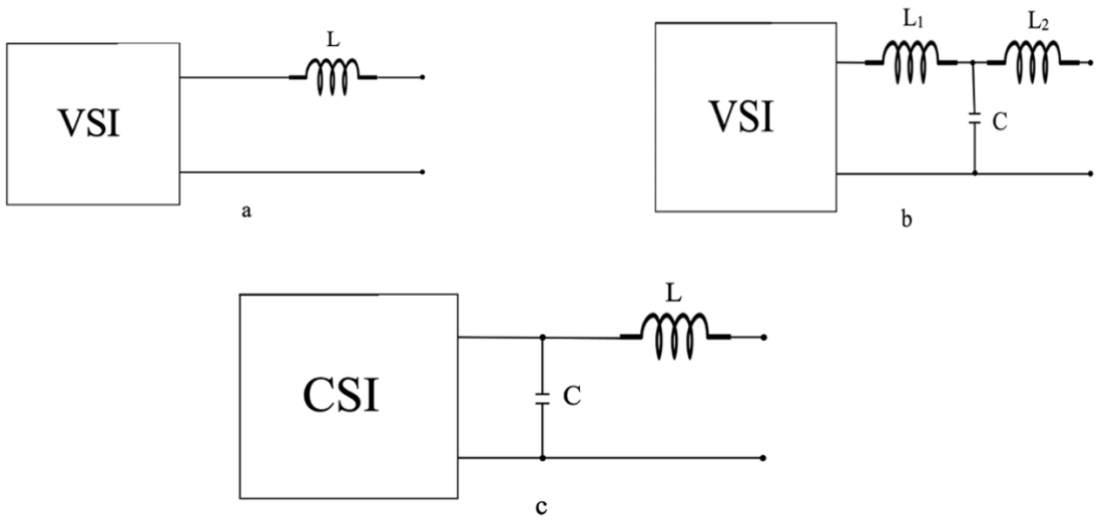

Figure 3.8 Low-pass filter types: L and LCL filters are for VSI, while the CL filter is for CSI.

In a case where the Q of the filter is too high, a rise in the THD can take place at the resonant frequency of the filter. In the opposite case, if the Q is too low, it will exhibit substantial filter loss. The suggested values of Q for a low-pass grid filter varies between 2-4 [44]. The CL-filter, as depicted in Figure 3.8c, is a second order filter that consists of one capacitor and one inductor. The CL filter can substantially attenuate the high-frequency PWM harmonics if the resonant frequency is selected to be small compared to the PWM f_{sw} (say, an order of magnitude lower). And it generally has better damping behaviour than an L-filter. If the resonant frequency is low, the low-pass filter requires a large filter inductance, which results in higher loss. On the other hand, if the f_{sw} is too high, switching losses are increased. In general, a properly designed filter should have the following characteristics:

- Minimum voltage drops across the filter.
- Minimum stored energy in the filter.
- Minimum reactive power injection and high-power factor operation.
- Improved damping performances.
- Low electromagnetic interference.
- Robust to parameter variations due to aging.
- Robust to external parameter variations such as the grid impedance.

Chapter 4

4 Control strategy of the three-phase current source inverter

The chapter will take a comprehensive look and discuss the various components functions and control strategies in detail, such as the choice of control type, controller optimization, control signal reference frames, PWM, and control systems of CSI in grid-connected mode. The control system of a grid-connected inverter is responsible for managing the power injection into the grid, obtained from a distributed generator. The main target for grid-connected mode is to achieve good tracking of controlled variables with minimal phase error. The tracking precision is constrained by the maximum allowable inverter switching frequency, the DC link voltage, and the converter output inductance. The main control for CSI can be divided into two main sections, which are the input-side controller and the grid-side controller. Input side controller:

- The main feature is to derive the maximum power from the input power source.
- Provide protection for the input-side converter.

Grid side controller:

- Grid synchronization is achieved by matching the voltage magnitude, phase angle, and frequency on the converter output and grid. (Known as grid-connected mode)
- Operate in island mode upon loss of grid power supply as a microgrid.
- Control of reactive power transfer between the power converter and grid.
- Control the quality of power injection into the grid.
- Load sharing of two parallel converters operating on the same microgrid.

The focus point in this thesis is the grid-side controller, thereby controlling the power injected into the grid. Some other PWM methods are used to control a CSI, such as carrier-based sinusoidal pulse-width modulation (CSPWM) [45] and space vector modulation (SVM) [46], [47]. DDPWM has been chosen for this thesis because it is a modulation strategy that is easy to understand, more intuitive than other PWM methods. The control system of a grid-connected CSI is built up from the integration of several components or subsystems, such as cascade control, PI-control, phase locked loop (PLL), park-transform, and PWM, as shown in the figure below.

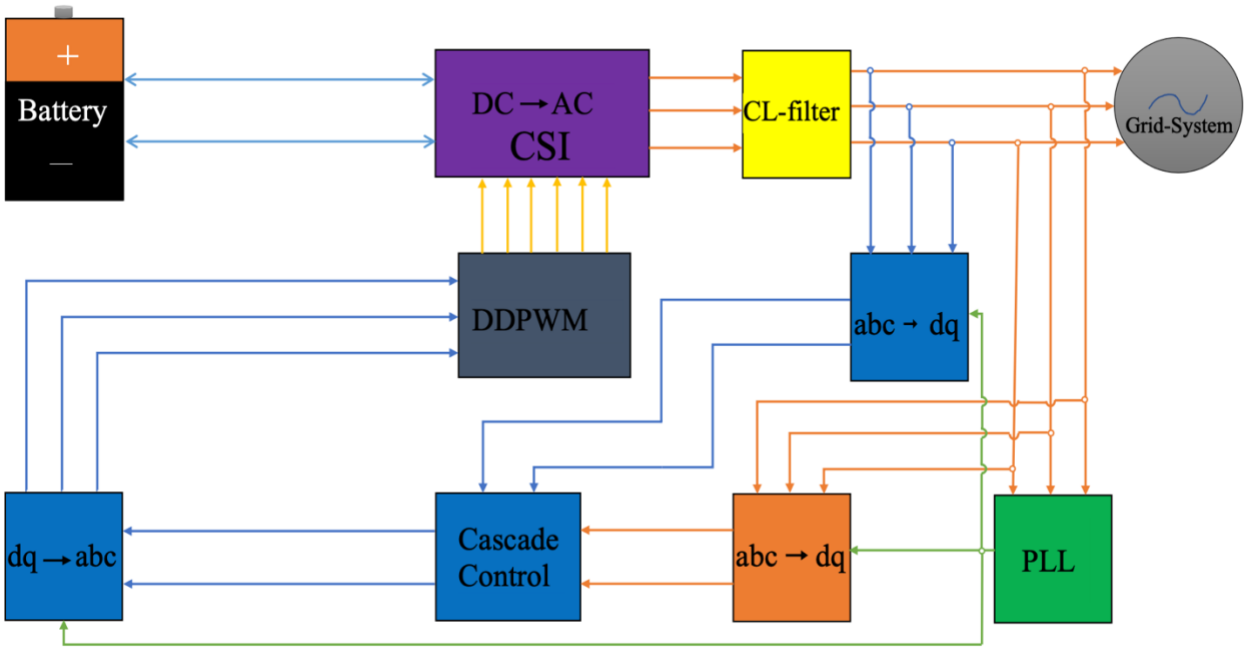

Figure 4.1 Block diagram of CSI based BESS.

4.1 Pulse width modulation

The PWM technique produces a sinusoidal waveform by filtering an output pulse waveform with varying width. A high switching frequency leads to a better filtered sinusoidal output waveform. There are three major PWM methods:

I. Carrier based PWM (CBPWM)
II. Programmed PWM (PPWM)
III. Space vector PWM (SVPWM)

The CBPWM is the most straightforward and simple of the three modulation techniques. The PWM technique for CSI is generally more challenging than the PWM technique for VSI. Many researchers have focused mainly on the two PWM methods, PPWM and SVPWM. The reason for CBPWM attracting less attention is that it requires what we called "sector" information to generate the actual gate signal, which makes it less intuitive. However, the real CBPWM for CSC hasn't been reported.

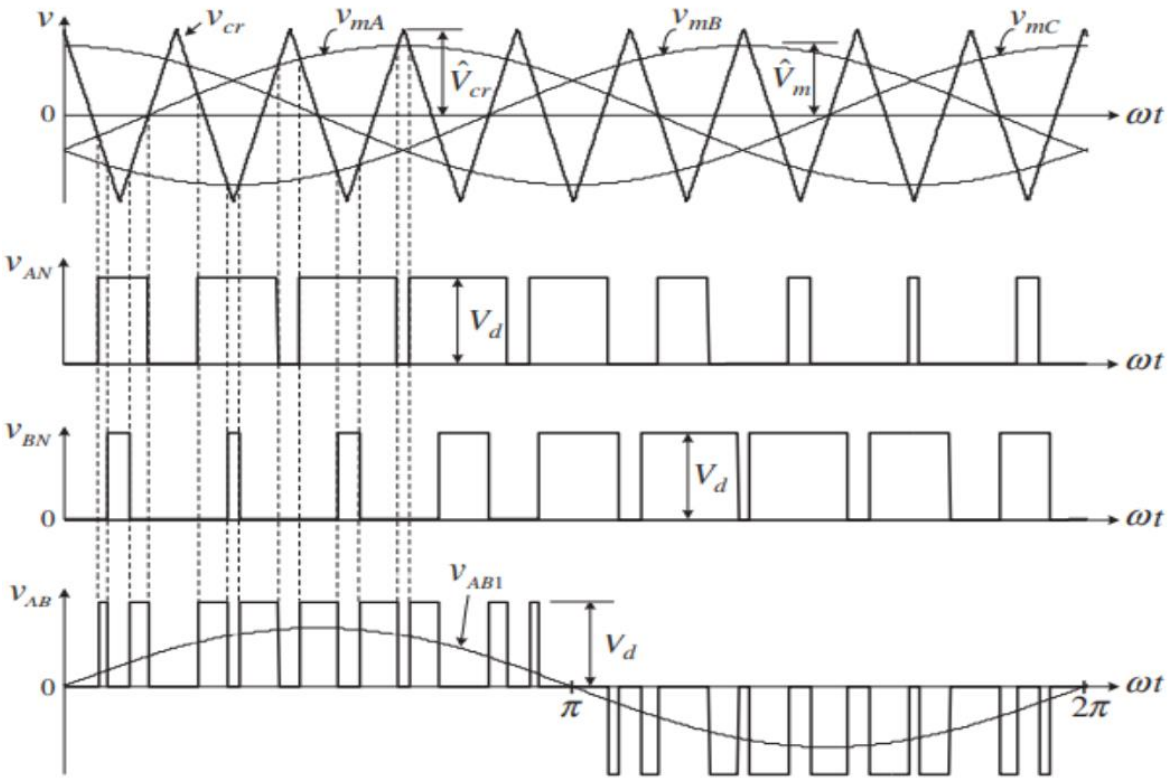

Figure 4.2 Sinusoidal Pulse Width Modulation [48].

The equations of amplitude modulation index and ratio of switching frequency are as follows:

$$m_a = \frac{I_m}{I_{dc}} \qquad (4.1)$$

$$m_f = \frac{f_{sw}}{f_0} \qquad (4.2)$$

Where are:

m_a The amplitude modulation index (where $0 \leq m_a \leq 1$)
I_m The peak phase current
I_{dc} DC-current
m_f The ratio of switching frequency
f_{SW} The switching frequency
f_0 The fundamental frequency

The choice of methods depends on the application's requirements, such as good waveform quality, high dynamic performance, low switching loss, and ease of implementation. Each of these three PWM techniques has its own advantages and disadvantages. The following are typical PWM inverter requirements:

- Wide range of linear operations.

- Minimum number of switches to maintain low switching losses in power components.
- Minimal content of harmonics in voltage and current because they produce additional losses and noise in the load.
- Elimination of low-frequency harmonics
- Operation in the overmodulation region, including square waves.

4.1.1 Direct duty-ratio pulse width modulation.

The three-phase CSI is proposed with a new DDPWM strategy. Three reference signals and two triangular carrier signals make up the proposed DDPWM for three-phase CSI. The fundamental procedure for producing the gate signals is the same as for the VSI.

The proposed DDPWM's block diagram is shown in Figure 4.3. In Figure 4.3, the three phase current commands ia*, ib*, and ic* are given, and the sorting comparator is used to select the maximum and minimum values of each command at each switching period. The suggested DDPWM method is an example of an open-loop control, so no feedback quantities are needed. It should be noted that when the suggested DDPWM is implemented, I_{DC} is a setting value rather than a measured value. The proposed PWM method for the three-phase CSC is illustrated in Figure 4.4 using an example where the amplitude modulation index (m_i) is 0.8 and the frequency modulation index (m_f) is 36. So, if the output frequency is 50 Hz, the carrier frequency will be 1.8 kHz. Notice that in Fig. 8, the a-phase current i_a has unipolar modulation during each half period [49].

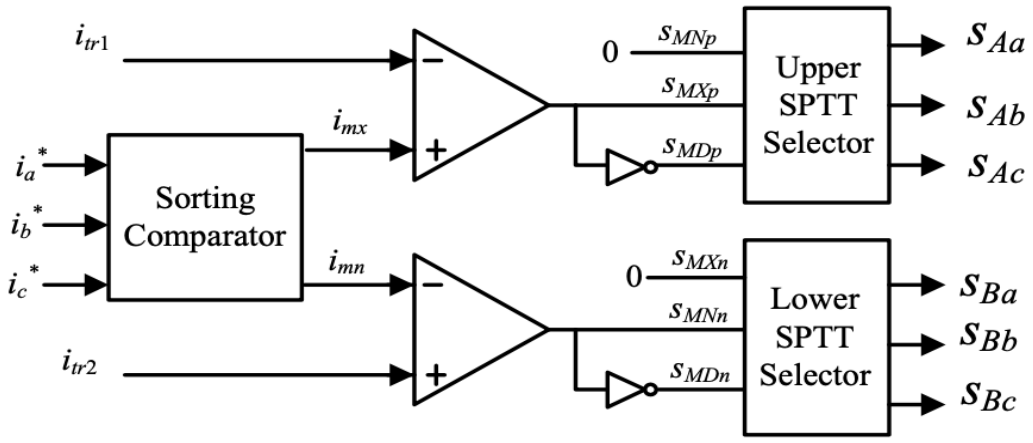

Figure 4.3 The block diagram of the proposed DDPWM [49].

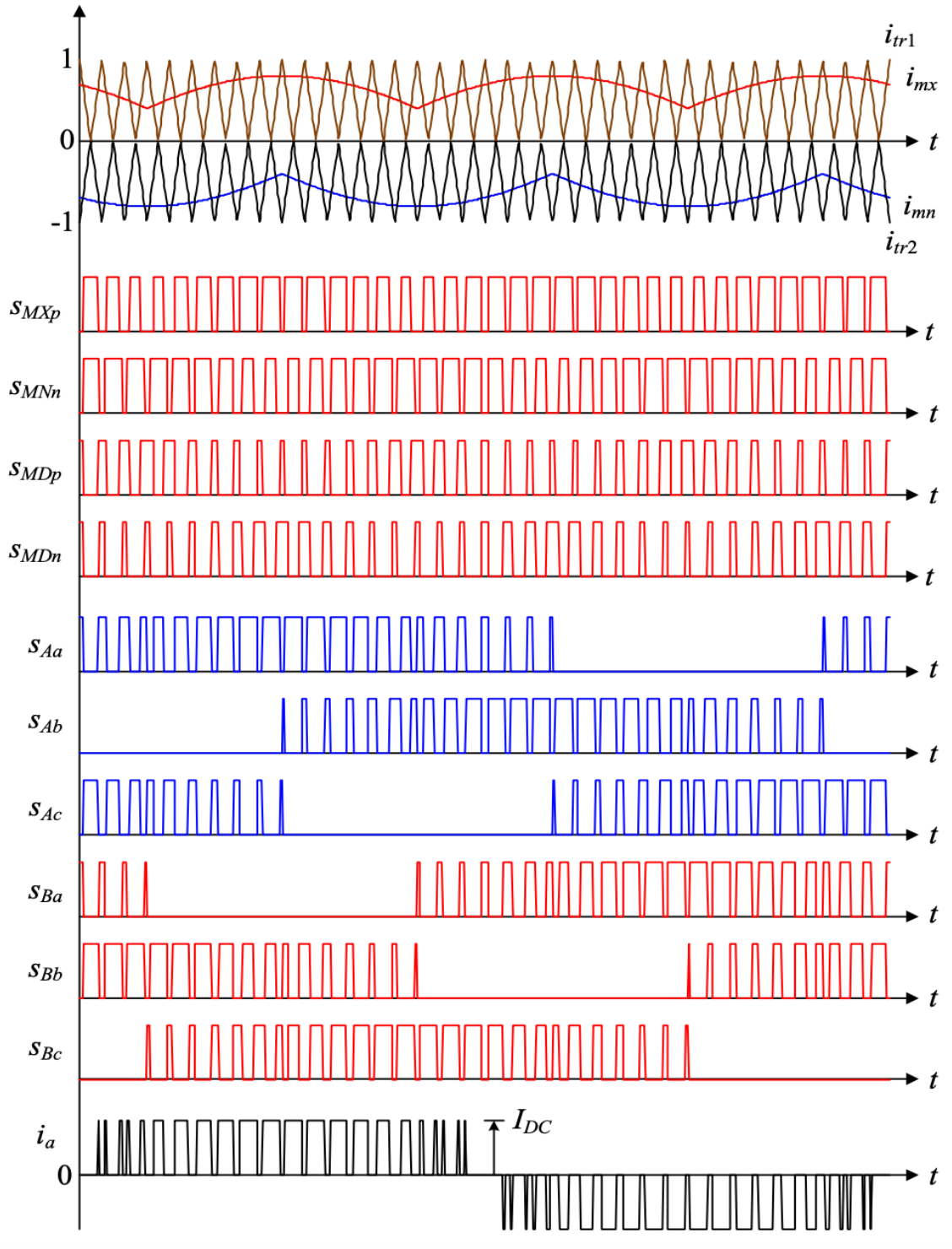

Figure 4.4 Generation of gating signals for the three-phase CSI [49].

The fundamental period T can be divided into 3 intervals, i.e., Min-, Mid- and Max-interval, according to the relative magnitude of a-phase command output current i_a^*. The effective switching frequency (f_{sw}) of the active switch can be estimated as follows:

$$f_{sw} \cong \frac{2}{3} f_c \qquad (4.3)$$

Where are:

f_{sw} Switching frequency
f_c Carrier frequency.

In this project, the DDPWM technique is used for the three-phase CSI because it is easy to understand and implement and more intuitive than other PWM methods such as PPWM and SVPWM. The operating principle and characteristics of DDPWM are discussed in previous work [49] .

4.2 Stationary ABC reference frame

The three-phase electrical system is a proven technology to generate, transmit, and distribute energy. But the drawback for the analysis of the three-phase system is that its oscillating nature may complicate the calculation, and three controllers are necessary in this case, one for each phase. The ABC phase quantities are transformed to the rotating dq0 reference frame by means of the park transformation. The dq0 frame rotates synchronously with the grid voltage, so that control variables become DC values. This makes filtering and controlling easier, and that is allowing us to use PI-controllers, as they have satisfactory behaviour when regulating DC variables [50]. Synchronous reference frame control is the most common method for grid-connected inverters. In this scheme, the inverter is controlled using a synchronous dq0 reference frame to inject a controlled current into the grid. The Park transformer transfers the ABC phase quantities to the dq0 reference frame.

4.3 Clarke and Park Transformation

The dq0 transformer is made of Park and Clarke transformation matrices. Park transformation, more often referred to as dq0-transformation, transforms three phase signals into a two-phase orthogonal system in a synchronous frame where the axis system is rotating on a reference frequency. This transformation requires a reference phase angle. But a three-phase voltage or current is first transformed into a two-phase signal (alpha-beta zero) by the Clarke transformation. And further, the $\alpha\beta 0$ system is transformed into dq0 system by the park transformation as shown in figure below gives an overview of the transformations. PWM needs a three phase AC-signal to operate, so the inverse Clarke and Park transformation converts the two DC-signals. The matrix components of the Clarke, Park, and inverse of these transformations for current, voltage and flux space vectors are summarized in table 4.1 and power calculations of these transformations are shown in table 4.2 below.

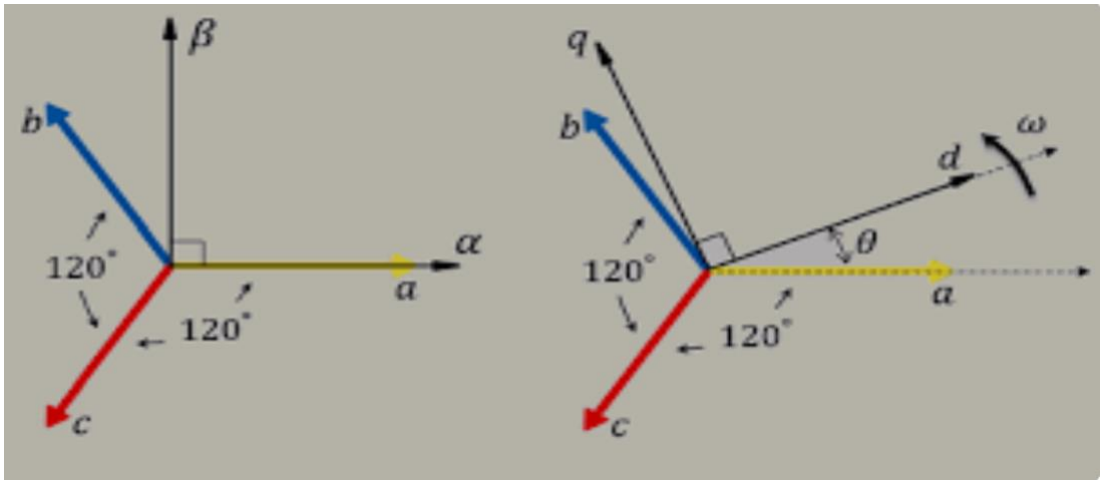

Figure 4.5 Left: ABC to αβ0 (Clarke transform), right: αβ0 to dq0 (Park transform) [51].

Table 4.1: Matrix transformation [48].

	Standard Amplitude-Invariant	Power-Invariant
Clarke *abc to αβ0*	$\frac{2}{3}\begin{bmatrix} 1 & -\frac{1}{2} & -\frac{1}{2} \\ 0 & \frac{\sqrt{3}}{2} & -\frac{\sqrt{3}}{2} \\ \frac{1}{2} & \frac{1}{2} & \frac{1}{2} \end{bmatrix}$	$\sqrt{\frac{2}{3}}\begin{bmatrix} 1 & -\frac{1}{2} & -\frac{1}{2} \\ 0 & \frac{\sqrt{3}}{2} & -\frac{\sqrt{3}}{2} \\ \frac{1}{\sqrt{2}} & \frac{1}{\sqrt{2}} & \frac{1}{\sqrt{2}} \end{bmatrix}$
Park *abc to dq0*	$\frac{2}{3}\begin{bmatrix} \cos(\theta) & \cos\left(\theta-\frac{2\pi}{3}\right) & \cos\left(\theta+\frac{2\pi}{3}\right) \\ -\sin(\theta) & -\sin\left(\theta-\frac{2\pi}{3}\right) & -\sin\left(\theta+\frac{2\pi}{3}\right) \\ \frac{1}{2} & \frac{1}{2} & \frac{1}{2} \end{bmatrix}$	$\sqrt{\frac{2}{3}}\begin{bmatrix} \cos(\theta) & \cos\left(\theta-\frac{2\pi}{3}\right) & \cos\left(\theta+\frac{2\pi}{3}\right) \\ -\sin(\theta) & -\sin\left(\theta-\frac{2\pi}{3}\right) & -\sin\left(\theta+\frac{2\pi}{3}\right) \\ \frac{1}{\sqrt{2}} & \frac{1}{\sqrt{2}} & \frac{1}{\sqrt{2}} \end{bmatrix}$
Inverse Clark *αβ0 to abc*	$\begin{bmatrix} 1 & 0 & 1 \\ -\frac{1}{2} & \frac{\sqrt{3}}{2} & 1 \\ -\frac{1}{2} & -\frac{\sqrt{3}}{2} & 1 \end{bmatrix}$	$\sqrt{\frac{2}{3}}\begin{bmatrix} 1 & 0 & \frac{1}{\sqrt{2}} \\ -\frac{1}{2} & \frac{\sqrt{3}}{2} & \frac{1}{\sqrt{2}} \\ -\frac{1}{2} & -\frac{\sqrt{3}}{2} & \frac{1}{\sqrt{2}} \end{bmatrix}$
Inverse Park *dq0 to abc*	$\begin{bmatrix} \cos(\theta) & -\sin(\theta) & 1 \\ \cos\left(\theta-\frac{2\pi}{3}\right) & -\sin\left(\theta-\frac{2\pi}{3}\right) & 1 \\ \cos\left(\theta+\frac{2\pi}{3}\right) & -\sin\left(\theta+\frac{2\pi}{3}\right) & 1 \end{bmatrix}$	$\sqrt{\frac{2}{3}}\begin{bmatrix} \cos(\theta) & -\sin(\theta) & \frac{1}{\sqrt{2}} \\ \cos\left(\theta-\frac{2\pi}{3}\right) & -\sin\left(\theta-\frac{2\pi}{3}\right) & \frac{1}{\sqrt{2}} \\ \cos\left(\theta+\frac{2\pi}{3}\right) & -\sin\left(\theta+\frac{2\pi}{3}\right) & \frac{1}{\sqrt{2}} \end{bmatrix}$

Table 4.2: Power transformation [48].

	Standard (Amplitude-Invariant)	Power-Invariant
$\alpha\beta0$	$p(t) = \frac{3}{2}(v_\alpha i_\alpha + v_\beta i_\beta + 2v_0 i_0)$	$p(t) = v_\alpha i_\alpha + v_\beta i_\beta + v_0 i_0$
	$q(t) = \frac{3}{2}(v_\beta i_\alpha + v_\alpha i_\beta)$	$q(t) = (v_\beta i_\alpha - v_\alpha i_\beta)$
$dq0$	$p(t) = \frac{3}{2}(v_d i_d + v_q i_q + 2v_0 i_0)$	$p(t) = (v_d i_d + v_d i_d + v_0 i_0)$
	$q(t) = \frac{3}{2}(v_q i_d - v_d i_q)$	$q(t) = (v_q i_d - v_d i_q)$

4.3.1 Phase-locked loop

Park transformations need to be synchronized with grids, and the PLL synchronizes the park transformations with grids in various algorithms. The phase angle for grid voltage is a critical piece of information for the systems that are coupled with the grid. This phase angle is used to control the flow of real and reactive power, switch on and off the power devices, and convert the control variables into suitable values by using a PLL [52]. The PLL block is made up of several components, as presented in Figure 4.6.

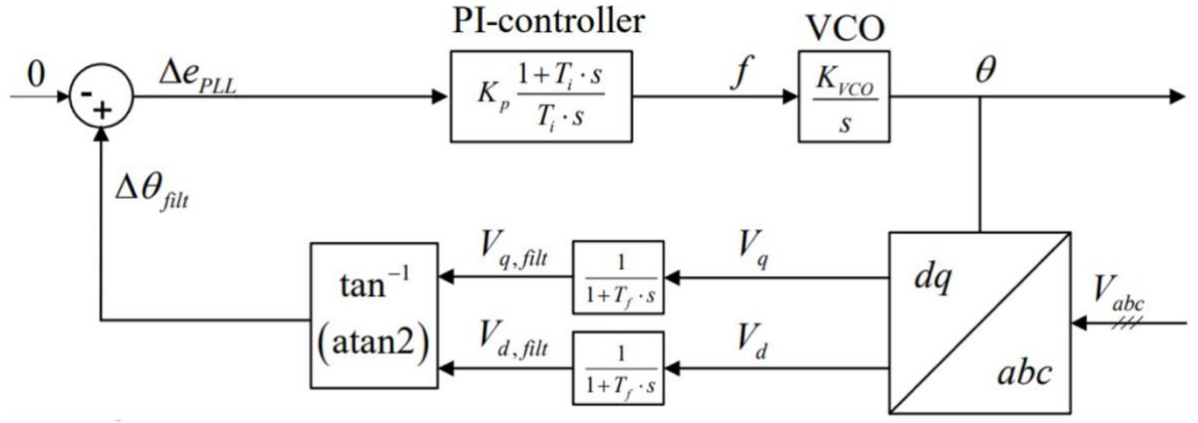

Figure 4.6 Block diagram of a PLL [52].

The PLL block may be divided into three main parts: a phase detector unit, a loop filter, and a voltage-controlled oscillator. The phase detector determines the phase difference between the input and the output signal. Then it feeds that signal to the loop filter unit to extract the DC component of the phase error. This DC component needs to be amplified before it goes into the PI-controller to generate the output signal frequency [50]. To form the phase angle, the output signal is integrated. When the output signals of the PLL are locked with the input

frequency, the phase difference from the phase detector unit will be 0. The purpose of the PLL control system is to accurately estimate the angle of the net victor of voltage by continuing to measure the three-phase instant voltage waveform. Moreover, the PLL provides good rejection of harmonics. Estimation of PLL angle is described in this work [52]. The transformation graph from ABC to αβ0, then from αβ0 to dq0 and the angle of PLL look as presented in Figure 4.7.

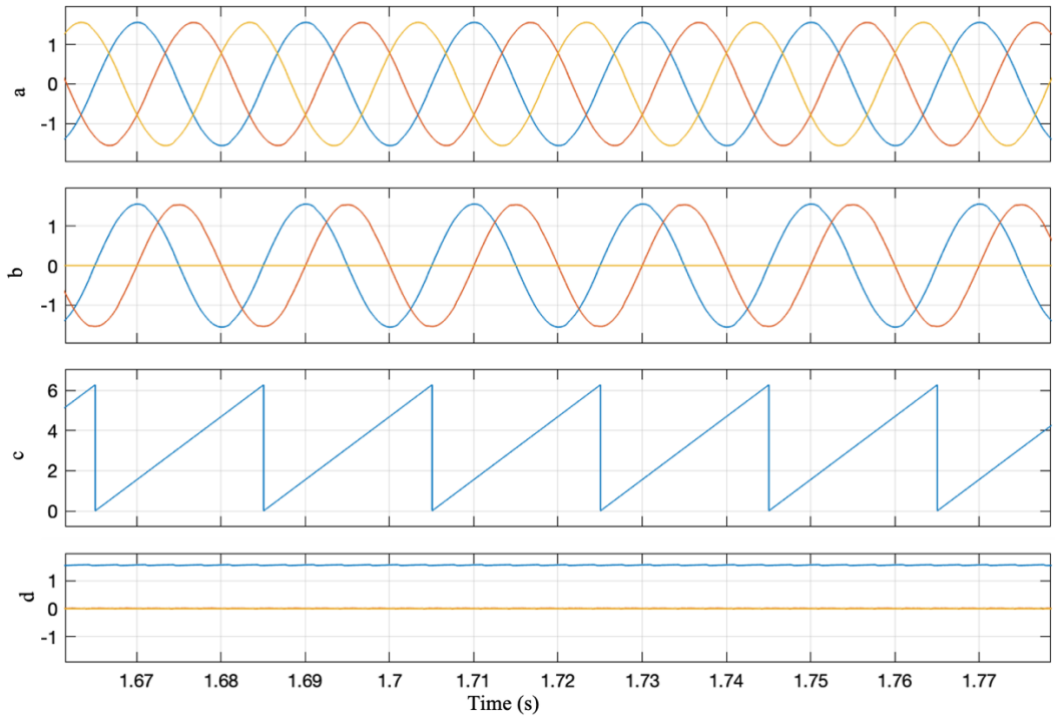

Figure 4.7 Transformations ABC to αβ0 and αβ0 to dq0, b αβ0 components, c PLL and d dq0 components.

4.4 Cascade control

The cascade controller is the main control for CSI, as illustrated in Figure 4.8. This model is the basis for the control strategy implemented in this project. Cascade control algorithms are constructed by two control loops: an inner loop with fast dynamics to eliminate input disturbances and an outer loop to regulate output performance. It is particularly useful when there are significant dynamic differences between the control and process variables, tight control actions can be achieved by using an intermediate signal that responds faster than the original control signal. It is difficult to obtain well-tuned PI parameters for both the outer loop and the inner loop simultaneously [53]. Cascade control has four PI controllers, and tuning four PI controllers is challenging. It is common to use the outer loop to regulate the current and the inner loop to regulate the voltage on the grid side of CSI. The inner control loop has a vital role in the overall dynamic responsiveness of a cascaded control structure. The important requirement for a cascaded control is that the bandwidth (speed of response) increase towards the inner loop, so the inner loop should be faster than the outer loop [54].

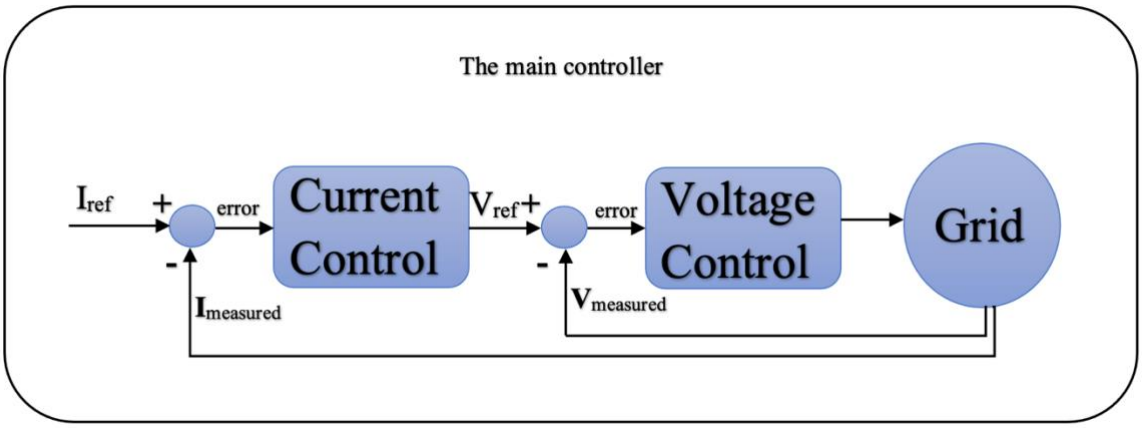

Figure 4.8 Generic block diagram of the cascade control system of grid-connected CSI

4.4.1 The inner loop

The voltage loop control is based on a reference/setpoint voltage input (v_{ref}). This v_{ref} is the output from the current loop, and the output of the inner loop control feeds to PWM. The controller performs reference tracking of the voltage, which ensures that the actual voltage is approximately equal to the reference voltage. The inner loop controller consists of two PI-controllers and two capacitor filters (the capacitor value must be the same value as the capacitor filter on the grid side of CSI), as shown in the figure below.

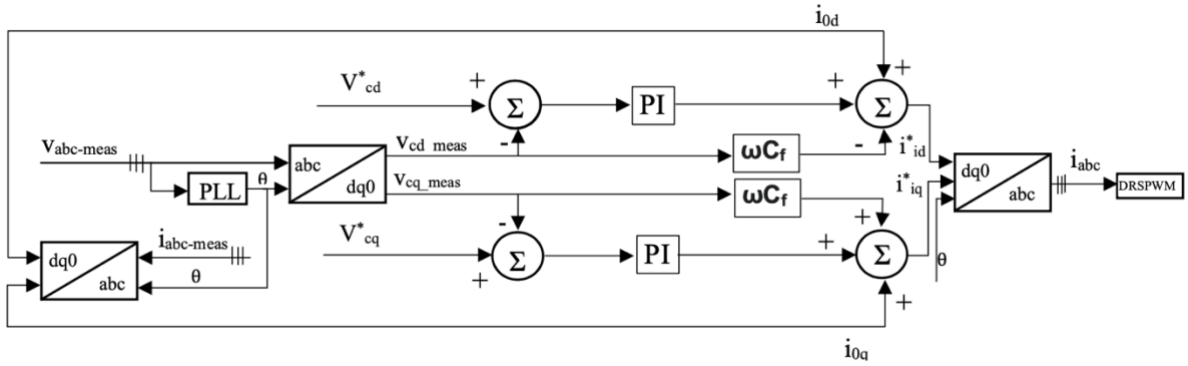

Figure 4.9 The inner control loop (voltage control loop).

4.4.2 The outer loop

The current loop control is based on a reference/setpoint current input (i_{ref}). This i_{ref} can be regulated manually or using a MPPT, and the output of the inductor loop control is the v_{ref} for the inner loop. The controller performs a reference tracking of the current, which ensures that the actual current (AC side current of CSI) is approximately equal to the reference current. The outer loop controller consists of two PI-controller like inner loops and two inductor filters (the inductor value must be the same value as the inductor filter on the grid side of CSI), as the figure below illustrates.

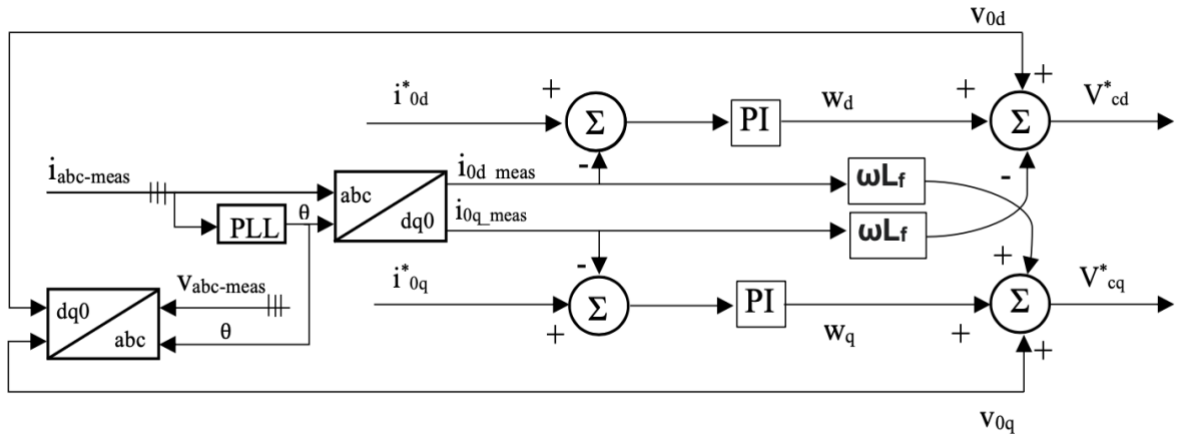

Figure 4.10 The outer control loop (current control loop).

4.4.3 Proportional integral controller

The PI-controller has several competitors [55], such as proportional-resonant control [56], hysteresis (on/off) voltage control, adaptive voltage control, and predictive control [57]. PI-controllers and proportional-resonant controls are commonly used to control the magnitude of the output voltage; they are flexible, have good harmonic rejection, have a fast response, and work well in grid-connected systems. In this project, a PI-controller is used to control and analyse the output active and reactive power of the CSI in grid-connected mode. The control variable is forced to track a time domain reference. The PI controller can achieve fast response and good harmonic rejection, when combined with a high inverter switching frequency. A compromise between reference tracking and stability is required in applications with a low switching frequency. However, the disadvantages of this controller are its inability to track a sinusoidal reference with zero steady-state error and poor disturbance rejection capability [58].

A PI regulator is widely used in industrial control systems. This is mainly due to the reduced number of parameters that need to be tuned. The PI controller is a linear controller; it works on the principle of control loop feedback, as depicted in Figure 4.11. The error of the reference and measured output signals is the function of the control response, which will regulate the output until it matches the reference value. There are two terms, namely proportional and integral action, in the PI controller.

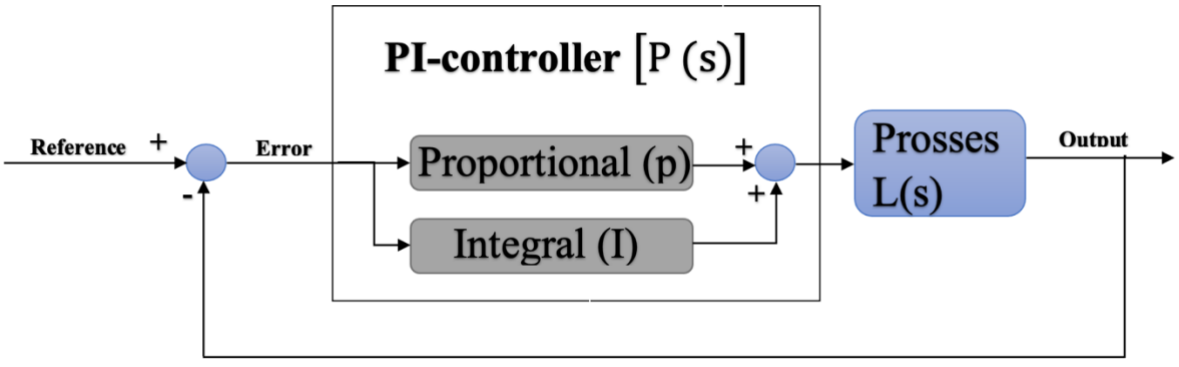

Figure 4.11 Generic system structure of PI-controller

4.4.3.1 Proportional action

The proportional action is simply proportional to the control error. The proportional term output is given by multiplying the error by a constant k_p which is the proportional gain constant. As the error becomes larger, the proportional term output of the controller is magnified to give more correction. A high k_p will produce a large change in output and may lead to system instability, while a low k_p will result in a less responsive controller to the system disturbance [59]. The equation of proportional action is given by 4.1.

$$U(t) = k_p * error(t) \qquad (4.3)$$

4.4.3.2 Integral action

The main objective of the integral term in a PI controller is to eliminate control error in steady state. The integral control is proportional to the magnitude and duration of the error. It calculates and accumulates a continuous sum of the error signal. Thus, a small steady-state error will result in a large error value over time. The accumulated error is then multiplied by the constant k_i, which is the integral gain constant and gives the integral control output. A small positive error will always lead to an increasing control output, and vice versa [59]. The equation of proportional action is given by 4.2.

$$U(t) = k_i * \int_0^t error(t) \qquad (4.4)$$

The PI-controller output can be expressed as equations 4.3 and 4.4 below, where T_i is the integral time constant and its transfer function representation is 4.5.

$$U(t) = k_p \left(error(t) + \frac{1}{T_i} * \int_0^t error(t) \right) \qquad (4.5)$$

Where are:

$$K_i = \frac{K_p}{T_i} \qquad (4.6)$$

$$P(s) = k_p \left[\frac{1+T_i S}{T_i S} \right] \qquad (4.7)$$

4.4.3.3 Tuning of proportional integral controller

The tuning of the PI-controller is one of the most vital and challenging aspects of this project. In this thesis, eight gains need to be tuned: four proportional and four integral gains. Tuning is the process of setting optimal values for proportional and integral gains to get the best performance close to the ideal of the PI-controller. According to [60] and [61], There are various classical and modern methodologies for tuning an analog or digital PI-controller to achieve suitable parameters k_p and k_i control gain. Some of the common tuning methods of PI-controllers include:

- trial-and-error approach
- Use of the Bode Plot
- Pole location
- Use of modulus optimum and symmetric optimum
- Ziegler-Nichols methods

In this thesis, the second Ziegler-Nichols method is used to tune the PI controller. Because the second Ziegler-Nichols method is a simple, easy method, we can obtain well-tuned parameters as with other methods [62]. The tuning process for the second Ziegler-Nichols method gain to obtain the optimized control gain is following; Set the value of ki to zero and set the value of kp to the lowest possible value. Then increase the value of kp gradually until it reaches kmax, where the maximum value of kp results in a sustained oscillation. Next, set kmax as kp and increase the value of ki until an optimized time response is obtained for the control system. The output might still have noise oscillation even though it achieved optimized time response. If that is the case, maintain the ki and reduce the kp to minimize the noise and oscillation. When an output waveform with optimized time response and lower noise is obtained. Then the values of kp and ki are considered an optimized PI-control gain for the control system.

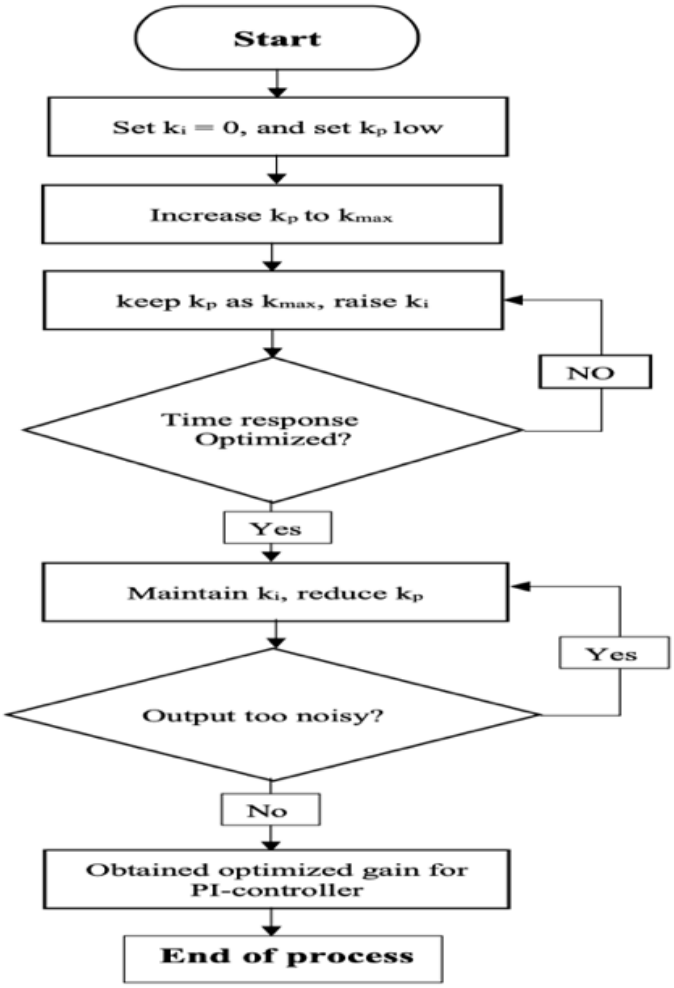

Figure 4.12 Block diagram tunning process of the second Ziegler-Nichols methods.

4.4.3.4 Tuning of cascade controller

As mentioned earlier, the tuning of cascade controllers is challenging work. The tuning process of the cascade controller in this project is as follows:

- Start tuning first with the inner control-loop.
- Set the value of ki equal to zero in both the inner and outer control-loop.
- Set the value kp very low in the outer control-loop.
- Once the inner control-loop is tuned, start the tuning of the outer control-loop.
- The tuning procedure for the PI-controller is described in the previous paragraph and can be followed.

4.5 Mathematical modelling of grid-connected CSI

In this section, the basic mathematical equations for controlling of three phase CSI in grid-connected systems are presented. Also describe more details of variable control and the manipulation of control variables to regulate AC-side of three-phase in grid-connected mode. This mathematical model is based on previous work [58]. The dynamic equations below describe the d-q axes of the CSI circuit based on Figure 3.4.

The dynamic equation in the dq-reference frame is the following:

$$\frac{di_{od}}{dt} = -\frac{R_F}{L_F} i_{0d} + \frac{(v_{0d} - v_{0q} + \omega L_F i_{oq})}{L_F} \quad (4.8)$$

$$\frac{di_{oq}}{dt} = -\frac{R_F}{L_F} i_{0q} + \frac{(v_{0q} - v_{0q} + \omega L_F i_{od})}{L_F} \quad (4.9)$$

$$\frac{dv_{od}}{dt} = \frac{(i_{id} - i_{0d} + \omega C_F v_{oq})}{C_F} \quad (4.10)$$

$$\frac{dv_{oq}}{dt} = \frac{(i_{iq} - i_{0q} - \omega C_F v_{od})}{C_F} \quad (4.11)$$

By assuming a fixed magnitude grid voltage, inverter active and reactive power exchange with the grid can be regulated directly by controlling the d-q components of the grid current. The reference current the CSI needs to inject into the grid at voltage $v_0 = v_{0d} + jv_{0q}$ to exchange specific active and reactive power can be expressed as:

$$\begin{bmatrix} i_{0d}^* \\ i_{0q}^* \end{bmatrix} = \frac{2}{3} \frac{1}{v_{0d}^2 + v_{0q}^2} \begin{bmatrix} v_{0d} & v_{0q} \\ v_{0q} & -v_{0d} \end{bmatrix} \begin{bmatrix} P^* \\ Q^* \end{bmatrix} \quad (4.12)$$

To assist the current regulator design, let
$w_d = v_{cd}^* - v_d + \omega L_F i_{oq}$ and $w_q = v_{cq}^* - v_q - \omega L_F i_{oq}$

Where the new variables w_d and w_q are obtained from the PI-controller as equation below:

$$w_d = k_p(i_{0d}^* - i_{0d}) + ki\int(i_{0d}^* - i_{0d})dt \quad (4.13)$$

$$w_q = k_p(i^*_{0q} - i_{0q}) + ki\int(i^*_{0q} - i_{0q})dt \qquad (4.14)$$

the integral parts of (4.13) and (4.14) are replaced with z_d and z_q and substituting the resultant expressions in (4.8) and (4.9), gives:

$$\frac{di_{od}}{dt} = -\frac{(R_F + k_p)}{L_F} i_{0d} + \frac{z_d}{L_F} + \frac{k_p}{L_F} i^*_{0d} \qquad (4.15)$$

$$\frac{di_{oq}}{dt} = -\frac{(R_F + k_p)}{L_F} i_{0q} + \frac{z_d}{L_F} + \frac{k_p}{L_F} i^*_{0d} \qquad (4.16)$$

$$\frac{dz_d}{dt} = ki(i^*_{0d} - i_{0d}) \qquad (4.17)$$

$$\frac{dz_q}{dt} = ki(i^*_{0q} - i_{0q}) \qquad (4.17)$$

We are rearranging the differential equations 4.15 to 4.17 to obtain in a form of state space formulation, $\dot{x}(t) = Ax(t) + Bu(t)$ as:

$$\frac{d}{dt}\begin{bmatrix} i_{0d} \\ z_d \\ i_{0q} \\ z_q \end{bmatrix} = \begin{vmatrix} -\frac{(R_F+K_p)}{L_f} & \frac{1}{L_f} & 0 & 0 \\ -k_i & 0 & 0 & 0 \\ 0 & 0 & \frac{(R_F+K_p)}{L_f} & \frac{1}{L_f} \\ 0 & 0 & -k_i & 0 \end{vmatrix} \begin{bmatrix} i_{0d} \\ z_d \\ i_{0q} \\ z_q \end{bmatrix} + \begin{vmatrix} \frac{k_p}{L_f} & 0 \\ k_i & 0 \\ 0 & \frac{k_p}{L_f} \\ 0 & k_i \end{vmatrix} \begin{bmatrix} i^*_{od} \\ i^*_{oq} \end{bmatrix} \qquad (4.18)$$

Where are:

i_{od} The d-component of measured current (v)
i_{oq} The q-component of measured current (v)
i_{id} Output current of control d-component (v)
i_{iq} Output current of control q-component (v)
V_{od} The d-component of measured voltage (v)
V_{oq} The q-component of measured voltage (v)
V^*_{cd} The reference for inner loop control of d-component voltage (v)
V^*_{cq} The reference for inner loop control of q-component voltage (v)
i^*_{od} Reference in d-component current (A)
i^*_{oq} Reference in q-component current (A)
P^* Active power (W)
Q^* Reactive power (VAr)
k_p Proportional gain (unit less quantity)
k_i Integral gain (unit less quantity)
C_f Filter capacitance (F)
L_f. Filter inductance (H)
ω Angular frequency (rad/s)
R_F Filter resistor (Ω)

w_d, w_q, z_d, & z_q are variables to simplify the voltage regulator design

The equation 4.18 shows the states related to the *d*-channel can be solved or controlled independent of the *q*-channel, hence decoupled control of active and reactive power is achieved.

Chapter 5

5 Simulation and discussions of results

This chapter starts with an introduction to the simulation program, converter ratings, and parameters, together with the synchronizing criteria implemented in the simulation work. Simulation results will be discussed and illustrated in this chapter. To validate the performance of the proposed control system for a three-phase power inverter, a simulation model of a three-phase grid-connected CSI with a control system has been developed. MATLAB/Simulink is used to simulate, analyse, and test the functionality of the control system for CSI. Some familiarity with MATLAB/Simulink is essential to understanding the simulation. Figure 4.1 shows a generic block diagram of the control system for three-phase grid-connected CSI.

5.2 Simulation of pulse-width modulation

As mentioned in the previous chapter, the PWM technique for CSI is more complex than the PWM for VSI. The PWM technique for CSI is more sophisticated and complex than the PWM technique for VSI. The PWM technique for CSI, as shown in the figure below, is based on previous work [49]. The PWM technique is tested for three different scenarios in CSI, including CSI without any kind of control system, standalone, and grid-connected. In these scenarios, it is very effective, and the result is what was expected. Figure 5.2 displays the outcomes of these PWM techniques.

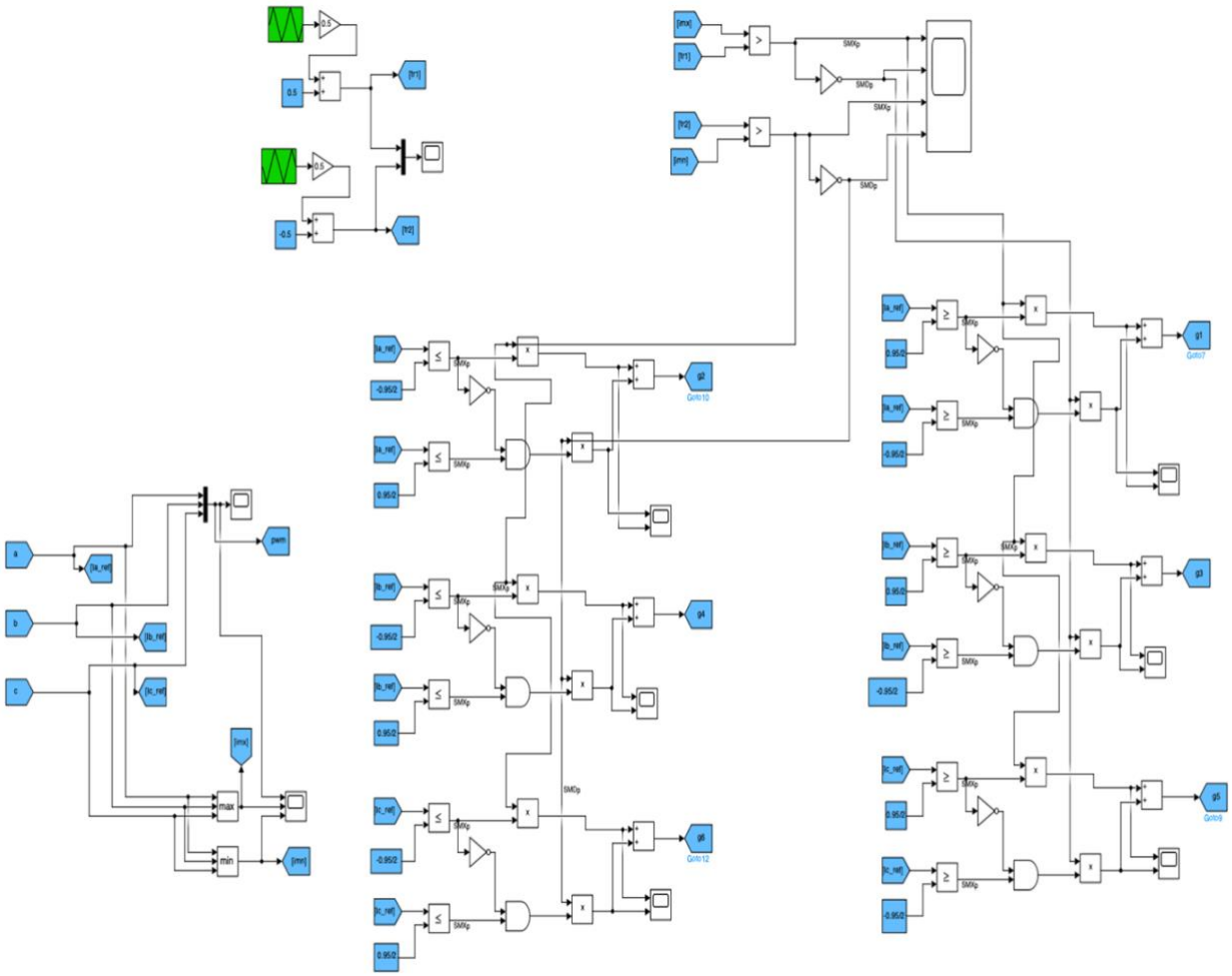

Figure 5.1 Block diagram technique of PWM.

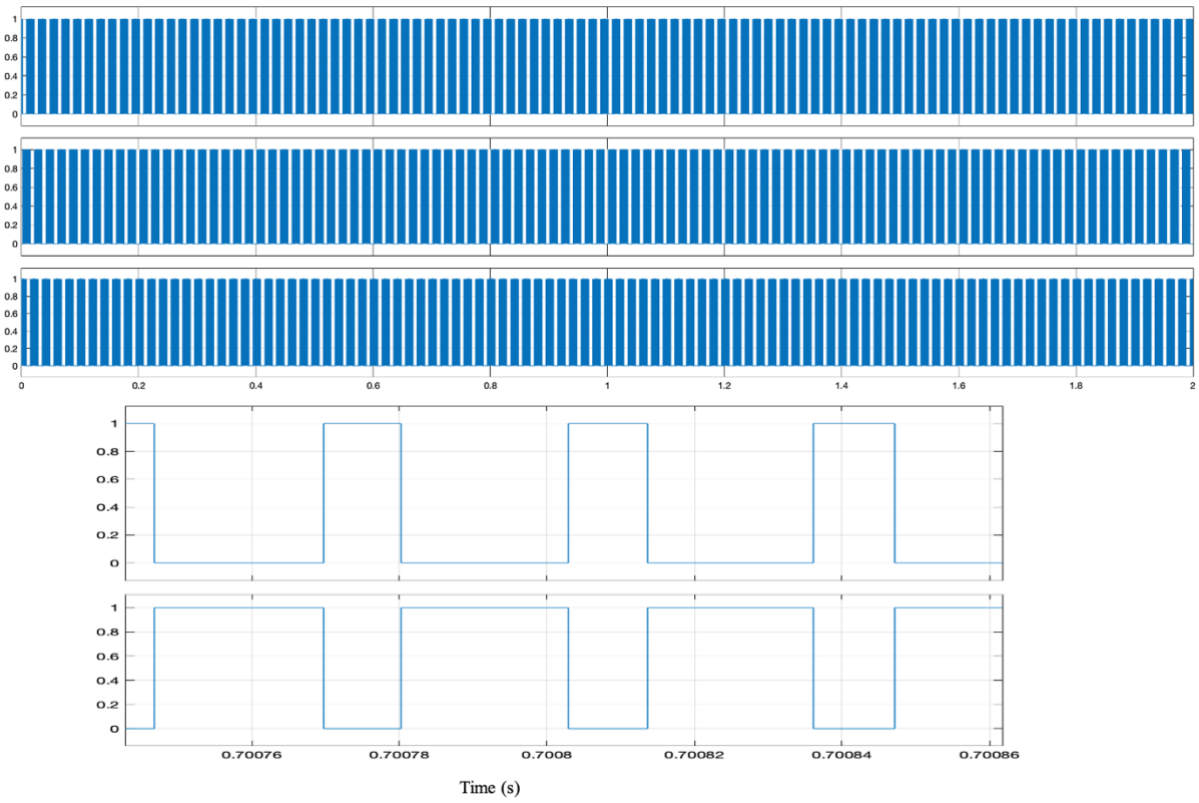

Figure 5.2 Output of PWM.

The output of PWM, which has a very nice amplitude and shape, is shown in Figure 5.2. Zoomed in three complete cycles, the PWM signal is neither under- nor over-modulated.

5.3 Voltage boosting capability of CSI

One of the advantages of CSI over VSI is that CSI has voltage-boosting capability. In this section discuss and show the results of testing the voltage boosting capability of CSI. Simulink has ideal current source, but to test for the voltage boosting capability of CSI, we must use a real voltage source. The parameters used for this test are shown in table 5.1.

Table 5.1 Parameters used in Voltage boosting capability of CSI.

Parameters		Values	SI units
DC-link (nominal) Voltage	(V_{dc})	200	v
Switching frequency	(f_s)	30	kHz
Line-to-line voltage	(Vca)	270	v
Filter capacitor	(C_F)	33	μF
Filter inductor	(L_F)	5	mH
Load	(R)	100	Ω

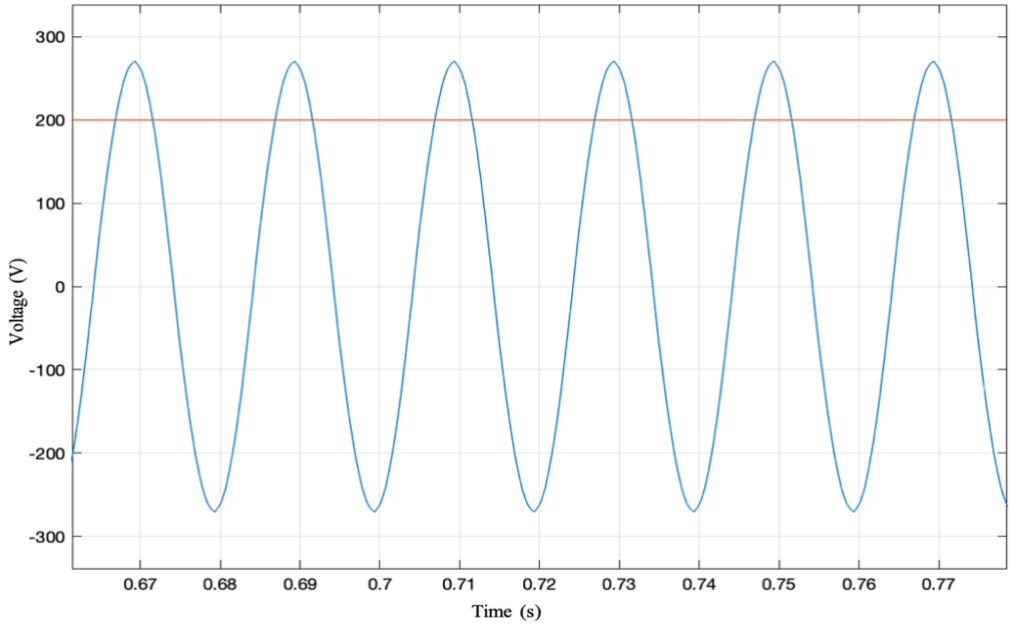

Figure 5.3 Voltage boosting capability.

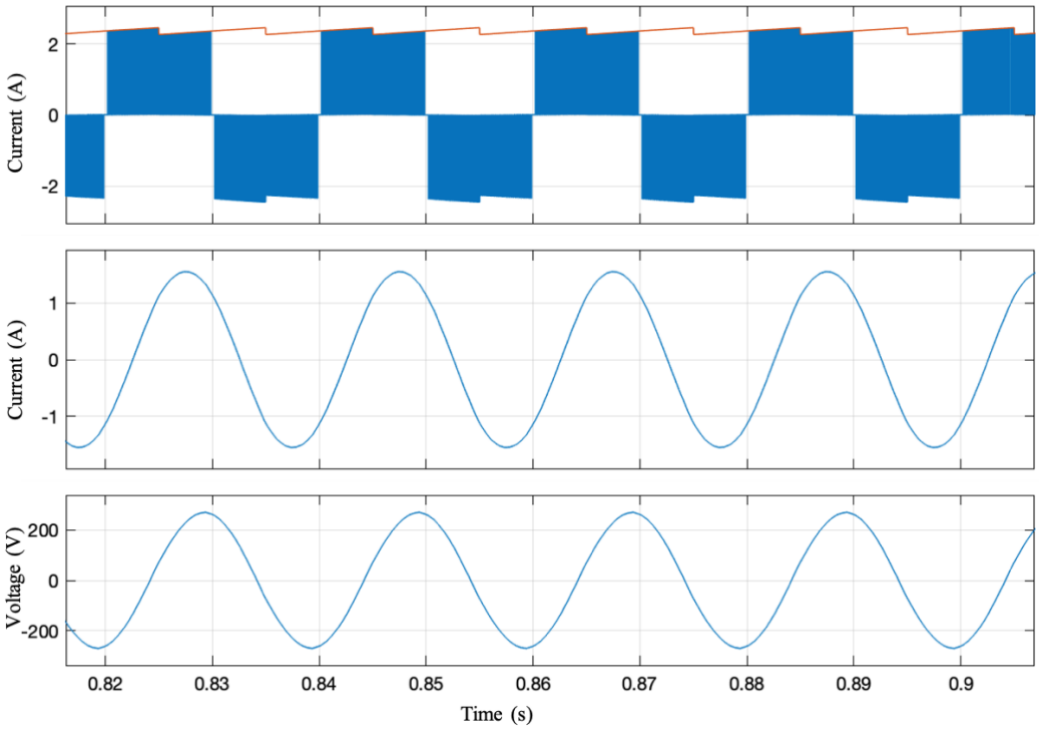

Figure 5.4 PWM and source current with a real source.

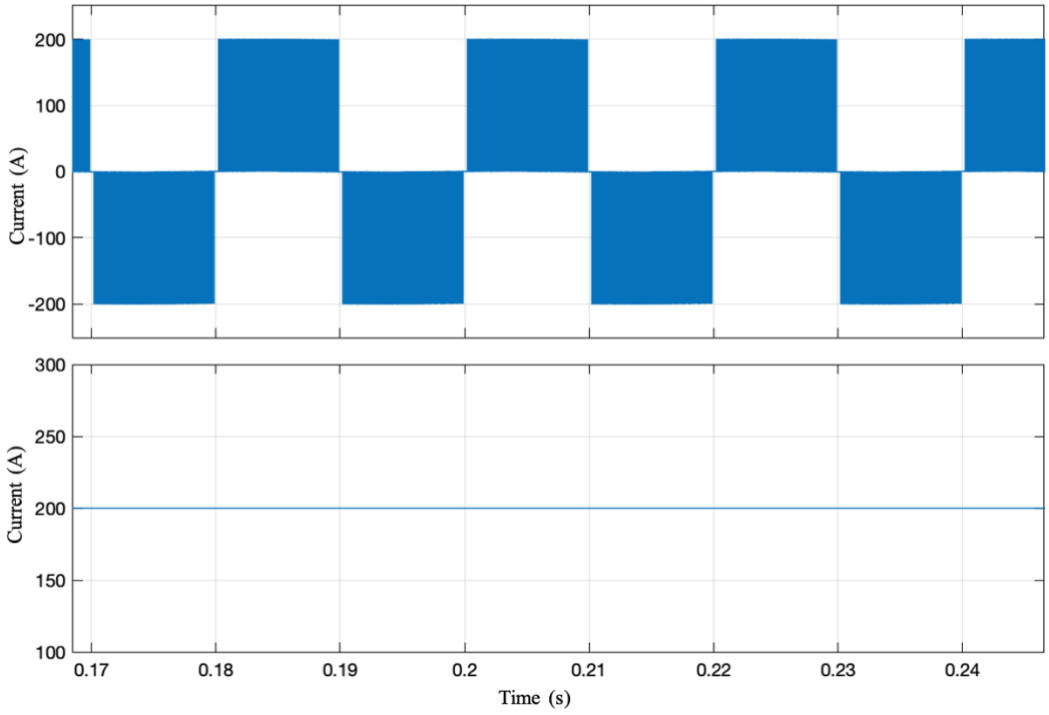

Figure 5.5 PWM and source current with an ideal source.

Figure 5.3 verifies that CSI has voltage-boosting capability. As we see from figure 5.3, the DC-link voltage is 200 v and the output voltage is 270 v. In figure 5.5, with an ideal current source, the PWM current looks good and doesn't have any ripples, but with an ideal current source, CSI has no voltage boosting capability. In figure 5.4, a real current source is used, and PWM current has ripples in this figure. The reason is the current source; as we see from the top of figure 5.4, the DC-link current has the same ripples, but we can remove these ripples with a filter.

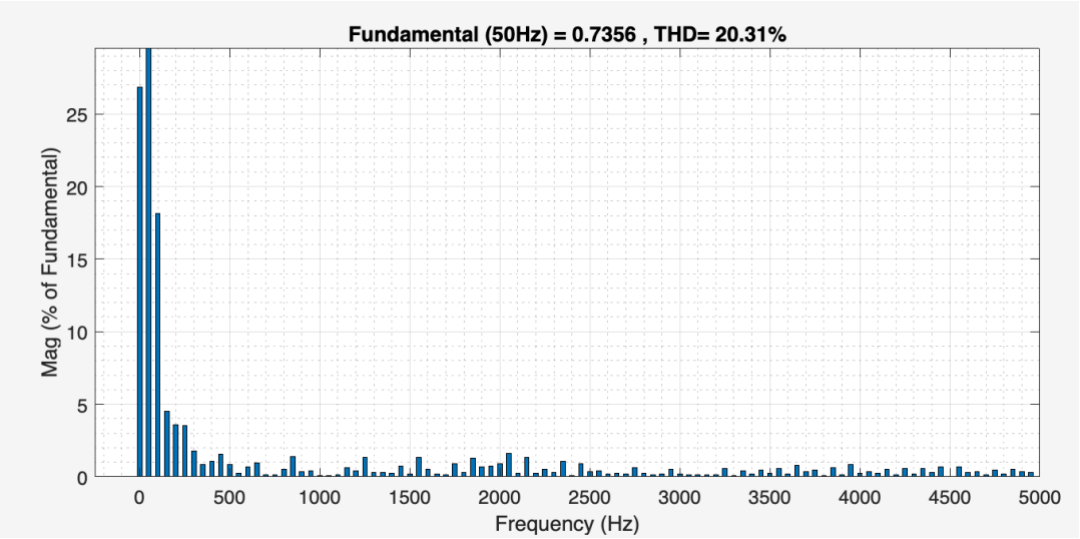

Figure 5.6 THD of current in a real current source.

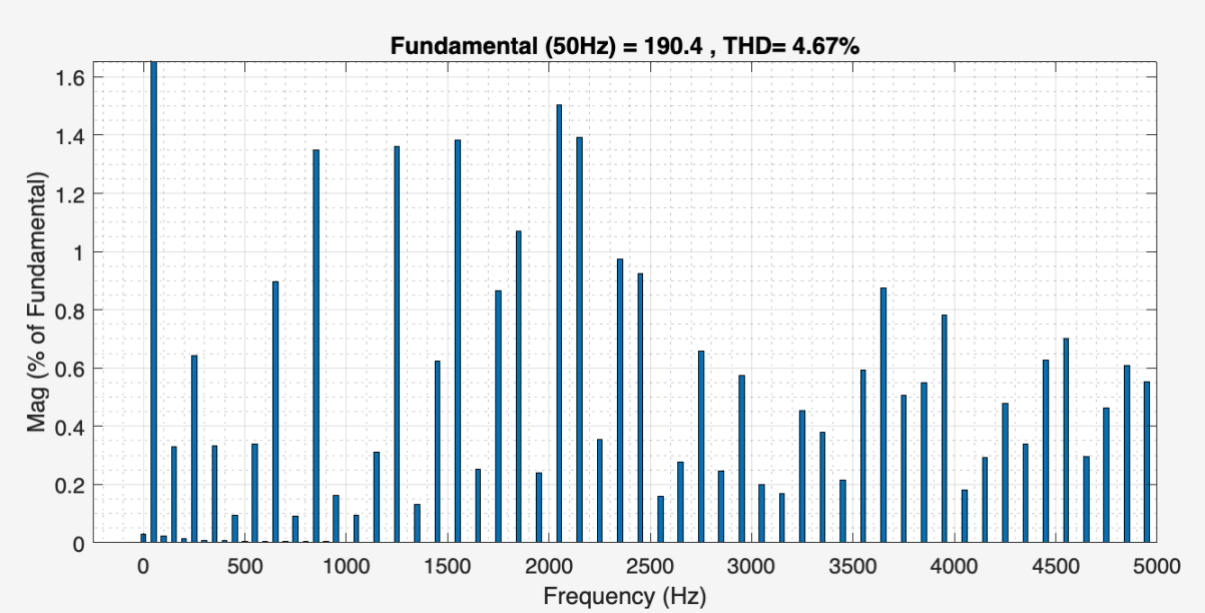

Figure 5.7 THD in the output AC current of CSI fed with ideal current source.

The THD is 4.67% in the output AC current of CSI fed with ideal current source, while the THD of current in a real current source is 20.31%. That is normal because the real current source has more noise than the ideal current source. These THD are illustrated in figures 4.6 and 4.7.

5.4 Simulation of current source inverter in grid-connoted

In this section, the results of simulation, used parameters, and discussion of three-phase grid-connected CSI are presented. Simulation of current source inverter in grid-connoted are in four main blocks have been used to simulate a three-phase CSI in grid-Connected. Each subsystem has several blocks and interconnecting lines. When we double-click on the subsystem block, we observe that Simulink displays all blocks, interconnecting lines, out-port, and in-port as shown in the figures below.

5.4.1 Parameters and per unit quantities

The express of a power-electronic converter system in a per-unit (pu) term, system rating, and filter parameters used for simulation and experimental results are listed in the tables below.

Table 5.2 Parameters used in simulation for grid-connected CSI.

Parameters		Values	SI units
DC-link (nominal) current	(I_{dc}) or (I_n)	20	A
Switching frequency	(f_s)	30	kHz
Line-to-line voltage	(Vca)	796	v
Nominal voltage	(V_n)	230	v
Filter capacitor	(C_F)	330	μF
Filter inductor	(L_F)	5	mH
Outer-loop controller proportional gain	(k_{pO})	(0.005)	unit less
Outer-loop controller integral gain	(k_{IO})	(0.004)	unit less
Inner-loop controller proportional gain	(k_{pI})	(0.12)	unit less
Inner-loop controller integral gain	(k_{II})	(0.009)	unit less

Table 5.3 Converter unit to per-unit system.

Parameters		Equations	Values	SI units
Base voltage (Peak phase voltage)	(V_b)	$V_b = \sqrt{\frac{2}{3}} V_{n,rms}$	187.79	V
Base current	(I_b)	$I_b = \sqrt{2} I_{n,rms}$	28.28	A
Base angular frequency	(ω_b)	$\omega_b = 2\pi f_n$	314.16	rad/s
Base impedance	(Z_b)	$Z_b = \frac{V_n}{I_n}$	6.64	Ω
Base inductance	(L_b)	$L_b = \frac{Z_n}{\omega_b}$	21.14	mH
Base capacitance	(C_b)	$C_b = \frac{1}{Z_b \omega_b}$	479.38	μF
Current per-unit	(I_{pu})	$I_{pu} = \frac{V_b \cdot 2\pi f C_f}{I_b}$	1	$unit$ less
Voltage per-unit	(V_{pu})	$V_{pu} = \frac{V}{V_b}$	1.23	$unit$ less
Inductance per-unit	(L_{pu})	$L_{pu} = \frac{L}{L_b}$	0.24	$unit$ less
Capacitance per-unit	(C_{pu})	$C_{pu} = \frac{C}{C_b}$	0.69	$unit$ less

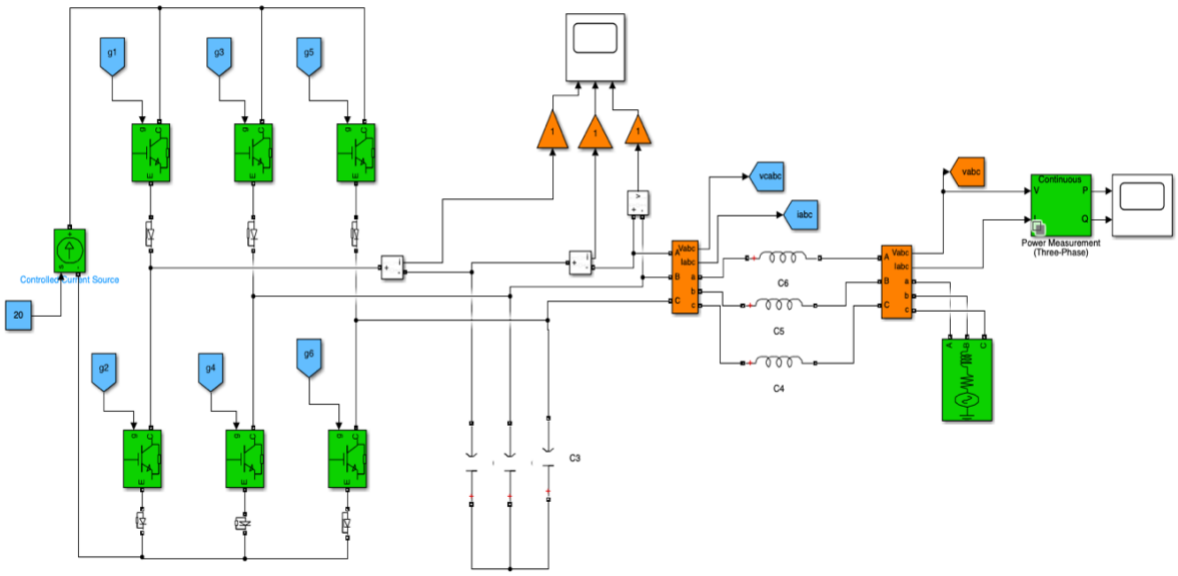

Figure 5.8 Simulation blocks of CSI.

For simulation of three-phase CSI in grid-connected systems, we used both real and ideal current sources, but in figure 5.9 is just a screenshot of an ideal current source.

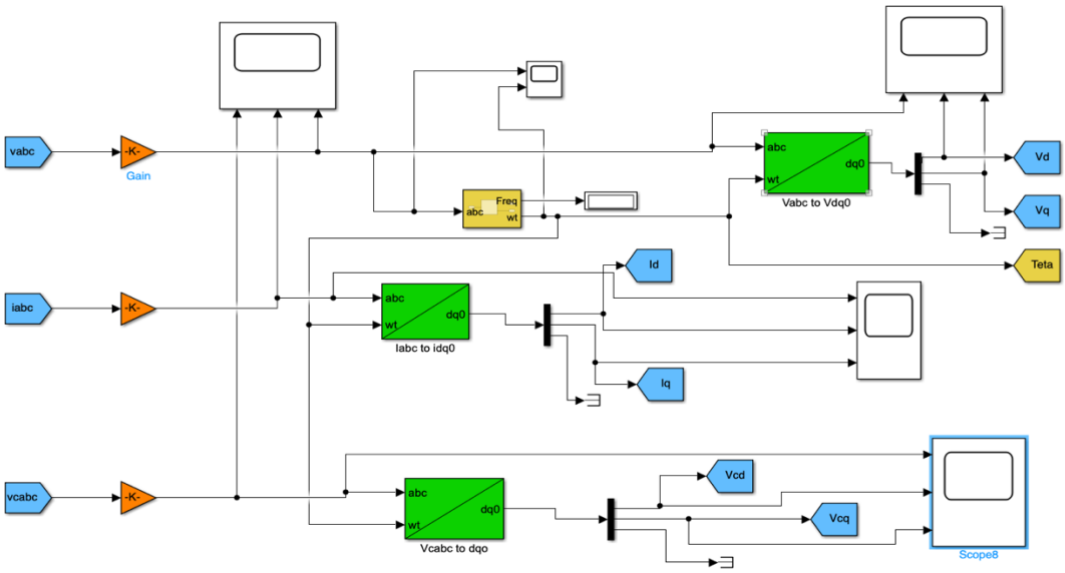

Figure 5.9 Simulation blocks of ABC to dq0 transformation.

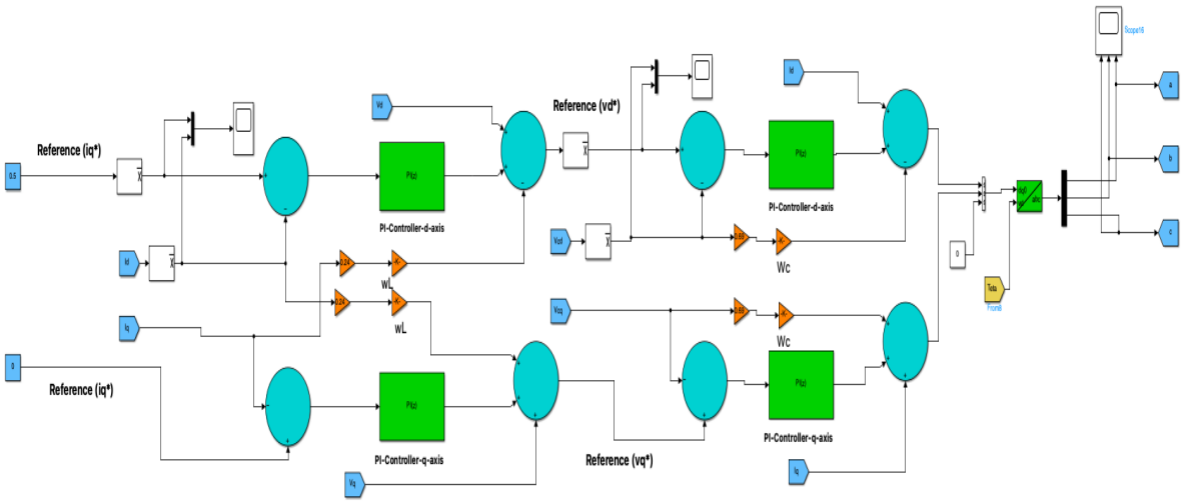

Figure 5.10 Simulation blocks of cascade-control.

We can see from the figures below that the output of CSI is as anticipated. The peak of PWM current is 20 A, like battery current at the source. The filter current, or sinewave current line-to-line, is close to 40 A. The output voltage line-to-line is almost 650 V, which means that the peak-to-peak voltage is 325 V and the R.M.S voltage will be 230 V. The voltage that CSI output should be 230 V. That show at the control system works as expected.

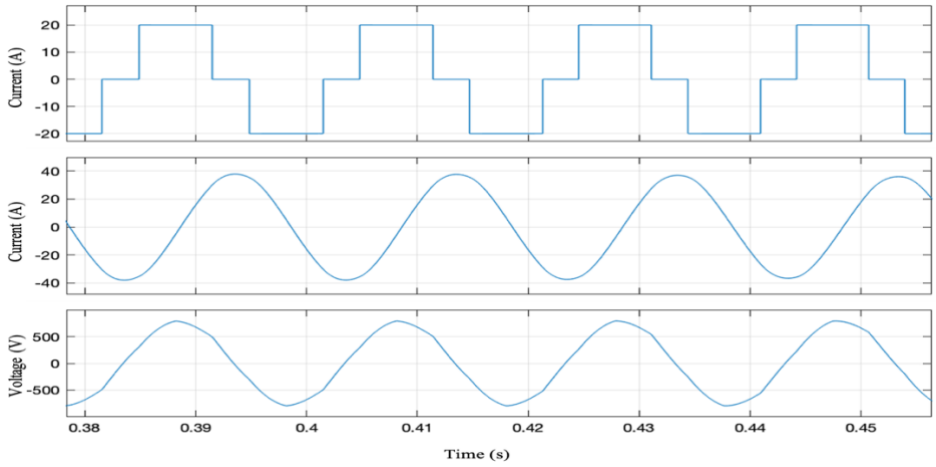

Figure 5.11 Output current and voltage of CSI.

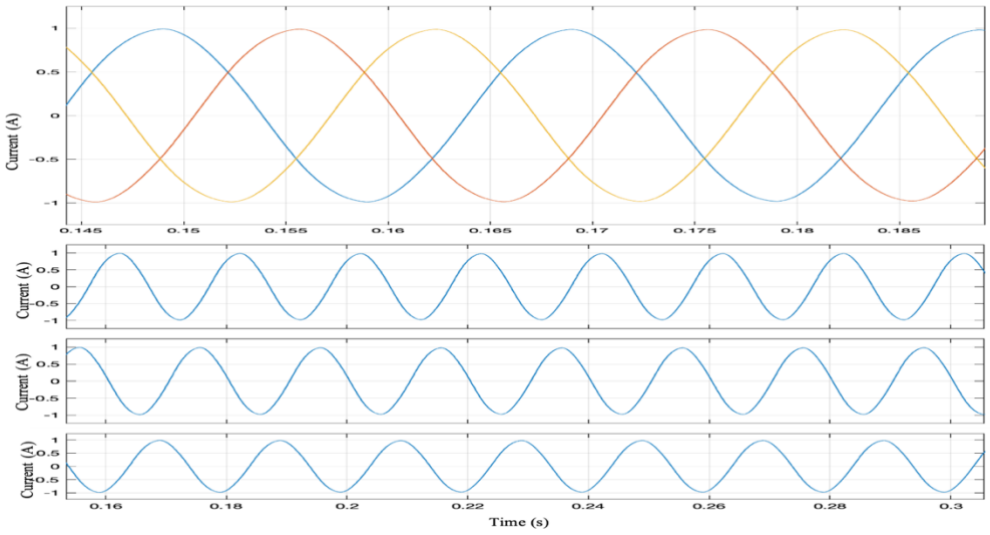

Figure 5.12 Output of cascade-control.

The output of cascade-control is a nice sinewave that is neither overmodulated nor under modulated; it is what is expected to be. This output is shown in the above figure.

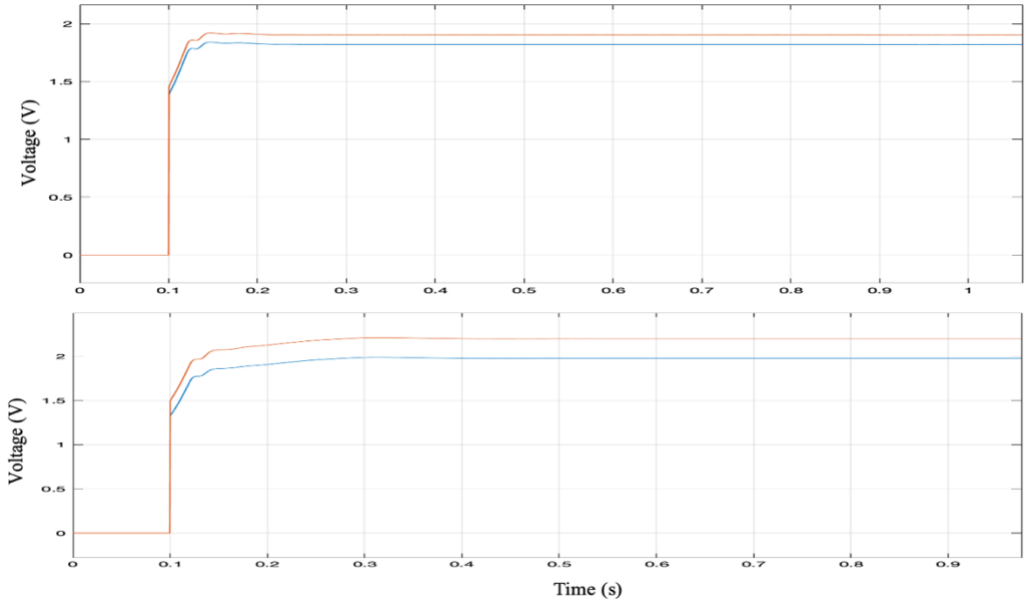

Figure 5.13 Static error of inner loop.

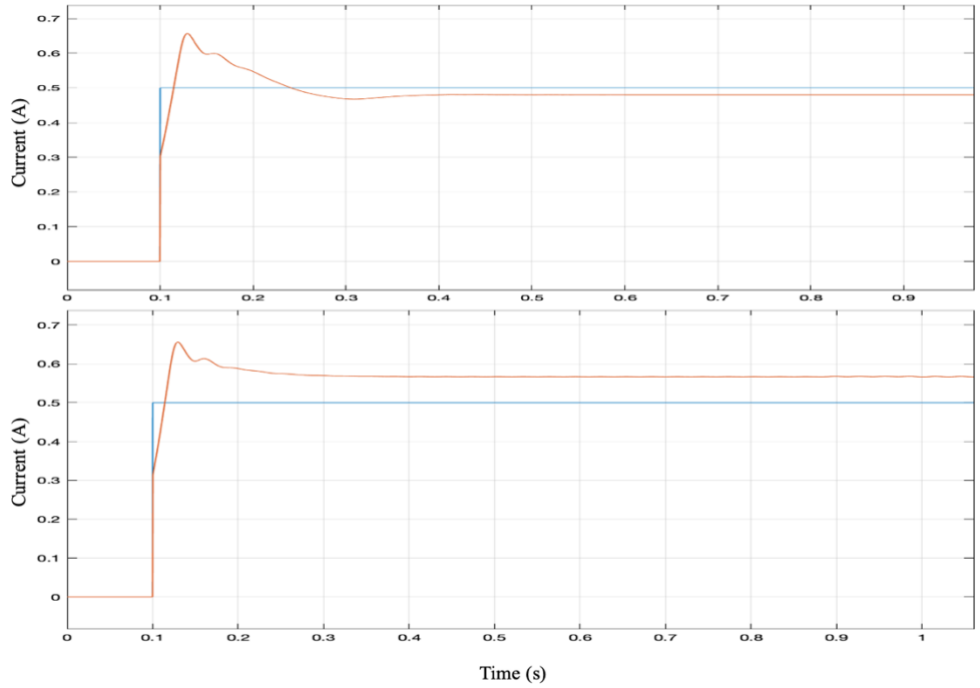

Figure 5.14 Static error of the outer loop.

The tuning of cascade control is a challenging process; in this simulation, several tuning methods have been used, such as Ziegler-Nichol's methods and auto-tuning. In both methods, the inner loop has been tuned first and the outer loop next. Either Ziegler-Nichol's methods or auto-tuning cannot get the static error to zero in both loops. When one loop gets closer to the reference value and the static error of another loop begins to increase, as shown in the graph above. But the most important thing is to track the measured value against the reference value, and it does.

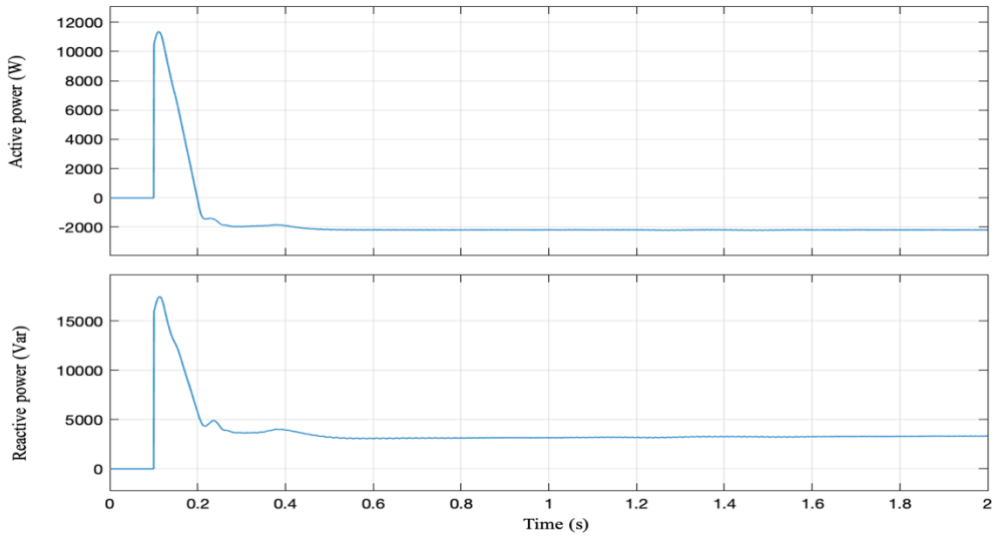

Figure 5.15 Active & reactive power.

The active and reactive powers behave a little strangely and need some improvement. Active power is expected to be negative, which it is, but reactive power is expected to be zero or close

to zero, which it isn’t. The active power enters a negative area when both integral gains are set to zero and both proportional gains increase, which means CSI is starting to inject power into the grid. But in this situation, the cascade-control system's outputs do not appear to be stable and are not in good shape. The supervisor suggested presenting it in its current form. Due to time constraints and the requirement for additional investigations.

Chapter 6

6 Conclusion and future work

The last chapter is divided into two sections, with the first section concluding the most important aspect of this thesis. While the second section proposes ideas for further work that can be done in future research, either within this thesis scope or out of it, for potential different control strategies and different topologies of CSI to be investigated.

6.1 Conclusion

The main goal of this work was to review the literature about CSI, design, simulate, analyse, and control the three-phase CSI in grid-connected systems. DDPWM is used as a PWM technique, and it works very well. The PI-control was chosen for this project because it is a simple to understand, it can improve the performance, stability, and accuracy of the system and has some degree of flexibility. Several subsystems make up the control system, including cascade-control (Voltage-control and current control), PLL, PWM, AC to DC transformer. The control system of three-phase CSI in grid-connected systems is theoretically modelled in Chapter 4. In Chapter 5, discuss the results of the simulation and show graphs of the simulation. The simulation worked, but it needs more investigation.

The focus of this thesis was three-phase CSI, but the rapport also gives a brief explanation of other related topics to CSI as well, such as renewable energy sources, challenges of global climate change, battery systems, and other necessary components for CSI to operate. All the descriptions of this are about how essential CSI is to convert DC to AC power, and CSI is playing an important role in reaching the climate target.

The task takes a comparative analysis between CSI and VSI to point out some important advantages and disadvantages of those converters, such as the fact that CSI has short-circuit protection and low switching loss, while VSI has open-circuit protection and low conduction loss. So, the conclusion is that both CSI and VSI have their own advantages and disadvantages, and the selection of inverter type depends on the requirements of the application, economic considerations, and its performance in varying environments. All in all, CSI is a serious competitor to VSI because CSI has some advantages over VSI.

In both current control and voltage control, an important observation is that by implementing feed-forward compensation of coupling components in the stationary αβ frame as applied in the dq synchronous frame, the steady-state error seems to be minimizing despite the more distorted three-phase filter current and voltage observed. In power-electronic converter systems, expressing voltage, current, impedance, and capacitance values on a per-unit basis makes the system simpler and produces a more accurate result. But the effect of this implementation requires more investigation for a solid conclusion.

Overall, the CSI is a strong rival for the VSI; all it requires is more research attention.

6.2 Recommendations for future work

As an extension of this study, the following topics are suggested:

- Test other control topologies to control the CSI, both grid-connected and standalone.
- Test different PWM techniques for CSI.

References:

[1] Shafiee, Shahriar, and Erkan Topal. "When will fossil fuel reserves be diminished?." Energy policy 37.1 (2009): 181-189.

[2] Morris-Suzuki, T., Boilley, D., McNeill, D., Gundersen, A., Beranek, J., Blomme, B., ... & Hirsch, H. Lessons from Fukushima-February 2012.

[3] Mara, Wil, and Carmen Bredeson. The Chernobyl disaster: legacy and impact on the future of nuclear energy. Cavendish Square Publishing, LLC, 2011.

[4] Agreement, Paris. "United nations framework convention on climate change, Paris, France." URL https://ec. europa. eu/clima/policies/international/negotiations/paris_en (2017).

[5] International Energy Agency. “Ch. 3: Energy, emissions and universal access”. In: World Energy Outlook 2017 1.1 (2017), pp. 107–152.

[6] Parker, Carl D. "Lead–acid battery energy-storage systems for electricity supply networks." Journal of Power Sources 100.1-2 (2001): 18-28.

[7] Rickard Östergård "Flywheel energy storage-a conceptucal study" Teknisk-naturvetenskaplig fakultet UTH-enheten pp. 45 - 2011

[8] Dai J, Xu D, Wu B. A novel control scheme for current-source-converter-based PMSG wind energy conversion systems. IEEE Transactions on Power Electronics. 2009; 24(4):963-72.

[9] Dash PP, Kazerani M. A multilevel current-source inverter based grid-connected photovoltaic system. In north american power symposium 2011 (pp. 1-6). IEEE.

[10] Wei Q, Xing L, Xu D, Wu B, Zargari NR. Modulation schemes for medium-voltage PWM current source converter-based drives: an overview. IEEE Journal of Emerging and Selected Topics in Power Electronics. 2018; 7(2):1152-61.

[11] Azmi, Syahrul Ashikin "Grid integration of renewable power generation" Department of Electronic and Electrical Engineering, University of Strathclyde, Ph.D. Thesis, 2014

[12] Kaushik Rajashekara, “Present Status and Future Trends in Electric Vehicle Propulsion Technologies,” IEEE J. Emerg. Sel. Topics Power Electron., vol.1, no.1, pp.3-10, Mar. 2013.

[13] Twining, Erika, and Donald Grahame Holmes. "Grid current regulation of a three-phase voltage source inverter with an LCL input filter." IEEE transactions on power electronics 18.3 (2003): 888-895.

[14] Woolaghan, Stephen. Current Source Inverters for PM Machine Control. The University of Manchester (United Kingdom), 2011.

[15] S.A. Azmi, M.A. Roslan, G.P. Adam and B.W. Williams. DC Current Offset Compensation Technique for Grid Connected Inverters, 9th International Conference on Power Electronics - ECCE Asia: Green World with Power Electronics (ICPE 2015-ECCE Asia) (2015) 617-623.

[16] A Vandermeulen and J. Maurin, Current source inverter vs, Voltage source inverter topology, (2014) 1–8.

[17] M. Mohr and F. W. Fuchs, "Comparison of three phase current source inverters and voltage source inverters linked with DC to DC boost converters for fuel cell generation systems," in 2005 European Conference on Power Electronics and Applications, 2005, pp. 1–10.

[18] M. Kazerani, Yang Ye, "Comparative evaluation of three-phase PWM voltage and current- source converter topologies in FACTS applications" IEEE Power Engineering Society Summer Meeting, 2002.

[19] K. P. Phillips, " Current-source converter for ac motor drives," IEEE Transactions Industry Applications, vol. 8, no. 5, pp. 679-683, Nov/Dec.1972.

[20] B.Mirafzal, M.Saghaleini and A.K.Kaviani, "An SVPWM-based switching pattern for stand-alone and grid connected three-phase single-stage boost-inverters," IEEE Trans. On Power Electron., vol.pp, Oct 2010.

[21] Cheng, Shu, et al. "An open-circuit fault-diagnosis method for inverters based on phase current." Transportation Safety and Environment 2.2 (2020): 148-160.

[22] Y.Suh, J.K.Steinke and P.K.Steimer, "Efficiency Comparison of Voltage-source and Current-source Drive Systems for Medium-Voltage Applications", IEEE Trans. of Ind.l Elect., vol.54, pp2521-2531, Oct. 2007.

[23] Fernandez, E., and M. Coello. "Control drive for SMPMSM in CSI converter with SiC devices." 2017 IEEE 37th Central America and Panama Convention (CONCAPAN XXXVII). IEEE, 2017

[24] Vazquez, S.; Lukic, S.M.; Galvan, E.; Franquelo, L.G.; Carrasco, J.M.; , "Energy Storage Systems for Transport and Grid Applications," Industrial Electronics, IEEE Transactions on , vol.57, no.12, pp.3881- 3895, Dec. 2010

[25] Joseph, Ami, and Mohammad Shahidehpour. "Battery storage systems in electric power systems." 2006 IEEE Power Engineering Society General Meeting. IEEE, 2006.

[26] Ioannis Hadjipaschalis, Andreas Poullikkas, Venizelos Efthimiou, "Overview of current and future energy storage technologies for electric power applications", Renewable and Sustainable Energy Reviews, Volume 13, Issues 6-7, August-September 2009, Pages 1513- 1522.

[27] D. Rastler. “Electricity Energy Storage Technology Options A White Paper Primer on Applications, Costs and Benefit”. Electric Power Research Institute 2009

[28] I. Gyuk. “EPRI-DOE Handbook of Energy Storage for Transmission and Distribution Applications”. U. S. Department of Energy.

[29] J. Jana, H. Saha and K. Das Bhattacharya, "A review of inverter topologies for single-phase grid-connected photovoltaic systems", Renewable and Sustainable Energy Reviews, vol. 72, pp. 1256- 1270, 2017.

[30] Antunes, Fernando Luiz Marcelo, Henrique Antônio Carvalho Braga, and Ivo Barbi. "Application of a generalized current multilevel cell to current-source inverters." IEEE Transactions on Industrial Electronics 46.1 (1999): 31-38

[31] S. B. Kjaer, J. K. Pedersen, and F. Blaabjerg, "A review of single-phase grid-connected inverters for photovoltaic modules," Industry Applications, IEEE, Transactions on, vol. 41, pp. 1292-1306, 2005.

[32] Kaviani, Ali K., and Behrooz Mirafzal. "A switching pattern for single-phase single-stage current source boost inverter." 2012 Twenty-Seventh Annual IEEE Applied Power Electronics Conference and Exposition (APEC). IEEE, 2012.

[33] S.A.Azmi, G.P.Ada and B.W.Williams, “New Modulation Strategy for Three-Phase Current Source Inverter,” 4th International Conference on Power Engineering, Energy and Electrical, pp.1110-1115, 2013.

[34] Azmi, S. A., et al. "Current control of grid connected three phase current source inverter based on medium power renewable energy system." International Journal of Advanced Technology and Engineering Exploration 8.74 (2021): 34-44.

[35] Patil, Nishad, et al. "Identification of failure precursor parameters for insulated gate bipolar transistors (IGBTs)." 2008 International conference on prognostics and health management. 2008, IEEE.

[36] H. Kim and K.-H. Kim, ”Filter design for grid connected PV inverters,” Proc. IEEE ICSET Conf., Singapore, Nov. 2008, pp. 1070-1075.

[37] IEEE1547-2003: "Standard for interconnecting distributed resources with electric power systems", IEEE, 2003

[38] IEEE Standard 929. IEEE Recommended Practice for Utility Interface of Photovoltaic (PV) Systems, 2000.

[39] M. Prodanovic and T. C. Green, "Control and filter design of three-phase inverters for high power quality grid connection," in IEEE Transactions on Power Electronics, vol. 18, no. 1, pp. 373 380, 2003.

[40] Ivanova, Elizaveta. Transient analysis of road tunnel power system. MS thesis. UiT Norges arktiske universitet, 2018.

[41] H. Kim and K.-H. Kim,"Filter design for grid connected PV inverters," Proc. IEEE ICSET Conf., Singapore, Nov. 2008, pp. 1070-1075.

[42] D. M. Whaley, "Low-cost small-scale wind power generation," Ph.D. dissertation, The School of Elect. and Electron. Eng., Univ. Adelaide, Adelaide, SA, Australia, Jul. 2009.

[43] Australia, Standard. "Grid connection of energy systems via inverters." Part 3: Grid protection requirements (2005): 7.

[44] M. Nave, Power Line Filter Design for Switched-Mode Power Supplies, 1st ed. New York: Springer, Jul. 1991.

[45] Espinoza, J.R., Joos, G.: 'Current-source converter on-line pattern generator switching frequency minimization', IEEE Trans. Ind. Electron., 1997, 44, pp. 198–206

[46] Dupczak, B.S., Perin, A.J., Heldwein, M.L.: 'Space vector modulationstrategy applied to interphase transformers-based five-level current source inverters', IEEE Trans. Power Electron., 2012, 27, pp. 2740–2751

[47] Azmi, Syahrul Ashikin, Grain Philip Adam, and Barry Williams. "New direct regular-sampled pulse-width modulation applicable for grid and islanding operation of current source inverters." IET Power Electronics 7.1 (2014): 220-236.

[48] Oladeji, Samuel, and Kazi Shoffiuddin Roni. Active Front End Converter with Virtual Damping and Inertia. MS thesis. NTNU, 2022.

[49] Choi, Nam-Sup, Kwang-Woon Lee, and Byung-Moon Han. "A novel carrier based PWM for current source converter." Proceedings of The 7th International Power Electronics and Motion Control Conference. Vol. 3. IEEE, 2012

[50] Blaabjerk, Frede, et al. "Overview of control and grid synchronization for distributed power generation systems." IEEE Transactions on industrial electronics 53.5 (2006): 1398-1409

[51] Hussein, Arkan A., Abdulbasit H. Ahmed, and Natheer M. Mohammed. "An enhanced implementation of SRF and DDSRF-PLL for three-phase converters in weak grid." International Journal of Emerging Electric Power Systems (2022).

[52] Storlien, Ole Amund. Comparison of droop-based grid-forming and PLL-based grid-following control of VSC during symmetrical fault. MS thesis. NTNU, 2022.

[53] G. Stephanopoulos, Chemical Process Control: An Introduction to the Theory and Practice. Englewood Cliffs, NJ: Prentice-Hall, 1984.

[54] Ashtiani, Nima Amouzegar, S. Ali Khajehoddin, and Masoud Karimi-Ghartemani. "Optimal design of nested current and voltage loops in grid-connected inverters." 2020 IEEE Applied Power Electronics Conference and Exposition (APEC). IEEE, 2020.

[55] M. Kazerani, Yang Ye, “Comparative evaluation of three-phase PWM voltage and current- source converter topologies in FACTS applications” IEEE Power Engineering Society Summer Meeting 2002.

[56] D.N.Zmood and D.G.Holmes, “Improved Voltage Regulation for Current Source Inverters,” IEEE Transaction on Industry Applications, vol.37, pp.1028-1036, 2011.

[57] H.F.Bilgin and M.Ermis, “Design and Implementation of A Current Source Converter for Use in Industry Applications of D-STATCOM,” IEEE Transcation on Power Electronics, vol.25, pp.1943-1957, 2010.

[58] A.Azmi, G.P.Adam and B.W.Williams, ”New Direct Regular Sampled Pulse Width Modulation Strategy for Current Source Inverter for Grid and Islanding Operation,” IET Transaction on Power Electronics,2013

[59] Low, Han Wee. "Control of grid connected active converter." MSc, Norwegian University of Science and Technology (2013).

[60] Kerdphol, Thongchart, et al. "Robust virtual inertia control of an islanded microgrid considering high penetration of renewable energy." IEEE Access 6 (2017): 625-636.

[61] R. Nilsen, “Electric Drives,” Course TET4120, Norwegian University of Science and Technology, NTNU, Trondheim, 2018.

[62] K. Astrom and T. Hagglund. PID controllers: Theory, design, and tuning. ISA: The Instrumentation, Systems, and Automation Society, 1995